

Free vibration analysis of sandwich structures reinforced by functionally graded carbon nanotubes

Alireza Pourmoayed^{*1}, Keramat Malekzadeh Fard^{2a} and Borhan Rousta^{3b}

¹Department of Mechanical Engineering, University of Khatamul-Anbiya Air Defense, Tehran, Iran

²Department of Aerospace Engineering, MalekAshtar University of Technology, Tehran, Iran

³Institute of Aviation Industry, Tehran, Iran

(Received May 20, 2020, Revised August 18, 2020, Accepted August 20, 2020)

Abstract. In this research, the behavior of free vibrations of sandwich structure with viscoelastic piezoelectric composite face sheets reinforced by Functionally Graded Carbon Nanotubes (FG-CNTs) and simply supported boundary conditions using a new improved higher-order sandwich panel theory were investigated. The viscoelastic sandwich structure is rested on viscoelastic foundation. There are 33 freedom degree based on higher order plate theories for top, center and bottom of the sandwich plate. To calculate exact solution, all of the stress components were engaged. The governing equations and boundary conditions were derived via the Hamilton's principle and finally, these equations solved by Navier's method. The accuracy of the present solutions is verified by comparing the obtained results with the existing solutions. The effect of different distributions of carbon nanotubes on non-dimensional natural frequency were inquired. Also, the effect of some important parameters such as those of length-to-thickness ratio and volume percentages of fibers, core thickness, elastic foundation, temperature and humidity changes, magnetic field, viscosity and voltage on free vibration response of sandwich structure were investigated.

Keywords: free vibration; sandwich structures; carbon nanotubes; viscoelastic foundation; piezoelectric

1. Introduction

Nowadays, sandwich structures vastly are used in aerospace, marine and automobile industries. Nano sandwich structures are the nanocomposite structures that are made of one or several materials with different shapes so that they result in lower weight, higher strength and good dynamic properties. Among these materials, polymeric sandwich nanostructures have higher performance and in various industries can be used. Also, in order to improve properties of mechanical, thermal and electrical various reinforces, including nanomaterials to these composite materials are added. In Mahi and Tounsi (2015), bending and free vibration analysis of isotropic, functionally graded, sandwich and laminated composite plates using a new hyperbolic shear deformation theory are presented. They accurate free vibration frequencies using a set of boundary characteristic orthogonal polynomials associated with Ritz method are calculated. In Ebrahimi and Farazmandnia (2018),

*Corresponding author, Assistant Professor, E-mail: pourmoayed@mut.ac.ir

^aProfessor, E-mail: kmalekzadeh@mut.ac.ir

^bPh.D., E-mail: Borhanrousta@yahoo.com

thermo-mechanical vibration of sandwich beams with a stiff core and face sheets made of functionally graded carbon nanotube-reinforced composite within the framework of Timoshenko beam theory is researched. They are shown that the vibration specifications of the curved nanosize beams are importantly influenced by the surface density effects. In Hadji *et al.* (2018), free vibrations analysis with stretching effect of nanocomposite beams reinforced by Single-Walled Carbon Nanotubes (SWCNTs) resting on an elastic foundation were studied. Natural frequencies are obtained for nanocomposite beams and then the effects of different parameters of the beam on the vibration responses of CNTRC beam are also considered. The bending and free vibration behavior of Functionally Graded Material (FGM) sandwich rectangular plates using an efficient and higher order shear deformation theory by Zouatnia and Hadji (2019) are investigated. In Hadji *et al.* (2011), free vibration analysis of Functionally Graded Material (FGM) sandwich rectangular plates using four-variable Refined Plate Theory (RPT) were investigated. In this study, the sandwich with the FGM face sheets and the homogeneous core and the sandwich with the homogeneous face sheets and the FGM core are considered. The fundamental frequencies by solving the eigenvalue problems are also extracted. In Emdadi *et al.* (2019), the free vibration analysis of annular sandwich plates with various functionally graded porous cores and carbon nanotubes reinforced composite face sheets based on modified couple stress theory and first order shear deformation theories were investigated. In Bellifa *et al.* (2016), bending and dynamic behaviors of functionally graded plates using a new first-order shear deformation theory are enlarged. They showed that the proposed theory is accurate and simple in solving the static bending and free vibration behaviors of functionally graded plates. An analytical method for vibrations of monolayer graphene plates on Pasternak foundation using the modified coupling stress theory by Akgöz and Civalek (2012) were obtained. A novel five variable refined plate theory for vibration analysis of functionally graded sandwich plates by Bennoun *et al.* (2016) is developed. In this study, by dividing the transverse displacement into bending, shear and thickness stretching parts, the number of unknowns and governing equations of the present theory is reduced, and hence, makes it simple to use. In Mohammadi *et al.* (2013), the non-local free vibrations of circular and hollow monolayer graphene plate on elastic foundation by differential squaring technique for different boundary conditions were studied. Their results showed that the natural frequency of these nano-plates with increasing small-scale coefficient for all boundary conditions were decreased. In Hadji and Safa (2020), the bending analysis of softcore and hardcore functionally graded sandwich beams using a new hyperbolic shear deformation theory were investigated. The effect of the deflections, stresses and sandwich beam type on the bending responses of functionally graded sandwich beams is discussed. In Murmu *et al.* (2013), the effect of plane magnetic field on transverse vibrations of graphene plate using the theory of equivalent nonlocal continuous environment mechanics were investigated. They showed that applying a magnetic field the natural frequency of the graphene plate increased. Buckling analysis with stretching effect of functionally graded carbon nanotube-reinforced composite beams resting on an elastic foundation by Khelifa *et al.* (2018) is investigated. SWCNTs are aligned and distributed in polymeric matrix with different patterns of reinforcement. In this research, the effects of different parameters of the beam on the buckling responses of CNTRC beam are also discussed. In Asgari *et al.* (2019), the dynamic instability of a three-layered, symmetric sandwich beam subjected to a periodic axial load resting on nonlinear elastic foundation was investigated. They showed that the responses of the dynamic instability of the system by the excitation frequency, the coefficients of foundation, the core thickness, the dynamic and static load factor were influenced. Wave propagation in functionally graded beams using various higher-order shear deformation beams theories by Hadji *et al.* (2017) were stretched. In this research, the effects of the volume fraction distributions on wave

propagation of functionally graded beam are also discussed. In Zouatnia *et al.* (2017), an analytical solution for bending and vibration responses of functionally graded beams with porosities are proposed. The Navier solution technique to derive analytical solutions for simply supported beams are pursued. In this study, the effects of the deflections, stresses and natural frequencies on the bending and free vibration responses of functionally graded beams are also studied. In Cheraghbak *et al.* (2019), free vibration of sandwich beam with flexible core resting on orthotropic Pasternak is investigated. In this research, the top and bottom layers by carbon nanotubes are reinforced and sandwich structural by Euler and Frostig theories is modeled. Thermal vibration analysis of FGM beams using an efficient shear deformation beam theory by Safa *et al.* (2019) were developed. The three cases of temperature distribution in the form of uniformity, linearity and nonlinearity through the beam thickness are considered. Then, the accuracy of solutions by comparing the obtained results with the existing solutions is validated. In Hadji and Bernard (2020), bending and free vibration analysis of functionally graded beams on elastic foundations with analytical validation are studied. The effect of different micromechanical models on the bending and free vibration response of these beams is also studied. They the effects of power-law index, length-to-thickness ratio, foundation parameter, the volume fraction of porosity and micromechanical models on the displacements, stresses and frequencies are also investigated. Static analysis of functionally graded sandwich plates with porosities based on high-order shear deformation theory by Keddouri *et al.* (2019) were studied. The effects of the material distribution, the sandwich plate geometry and the porosity on the deflections and stresses of FG sandwich plates are investigated. Hedayati and Aragh (2012) used three-dimensional elasticity method for vibration analysis of hollow plate reinforced with carbon nanotubes. They showed that the frequency in the symmetric distribution of carbon cumulative nanotubes more than the asymmetric and uniform distribution decreased. The bending and free vibration analysis of multilayered plates and shells by utilizing a new Higher order Shear Deformation Theory (HSDT) by Zine *et al.* (2018) are reported. In this study, bending and vibration results for cylindrical and spherical shells and plates for simply supported boundary conditions are also extracted.

This study investigated the free vibration analysis of sandwich structure with viscoelastic piezoelectric composite face sheets reinforced by functionally graded carbon nanotubes using a new improved higher-order sandwich panel theory. The sandwich structure is rested on viscoelastic foundation. The equations of motion for this sandwich structure using Hamilton's principle obtained and by Navier's method were solved. Then, influences of various parameters on free vibration of the sandwich structure were investigated. The results showed that considering magnetic field, external voltage and elastic foundation lead to increasing of the natural frequency.

2. Theory and formulation

2.1 Basic assumptions

The geometry of the sandwich structure with viscoelastic piezoelectric composite face sheets reinforced by functionally graded carbon nanotubes schematically are shown in Fig. 1. In this figure, indices a , b and h refer to the length, width and overall height of the sandwich structure, respectively. The sandwich structure on the viscoelastic foundation was located. Moreover, the top plate with index " t ", the bottom plate with index " b " and the central plate which is isotropic with index " c " are shown.

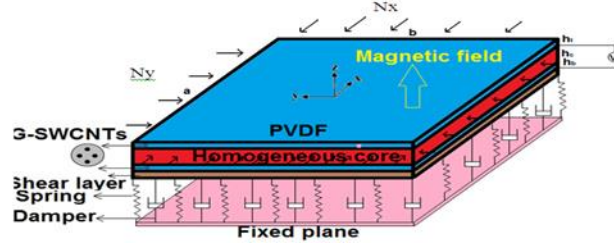


Fig. 1 Schematic of viscoelastic piezoelectric composite sandwich structures on viscoelastic foundation

2.2 Different distributions of single wall carbon nanotubes

The various distributions of single-wall carbon nanotubes that including *FG-O*, *FG-X*, *FG-V* and uniform distribution are were considered. The volume fraction of these four distributions is defined as follows.

$$V_{SWCNT} \begin{cases} V_{SWCNT}^* & UD \\ \left(1 + \frac{2z}{h}\right) V_{SWCNT}^* & FG - V \\ 2 \left(1 - \frac{2|z|}{h}\right) V_{SWCNT}^* & FG - O \\ 2 \left(\frac{2|z|}{h}\right) V_{SWCNT}^* & FG - X \end{cases} \quad (1)$$

where

$$V_{SWCNT}^* = \frac{w_{SWCNT}}{w_{SWCNT} + \left(\frac{\rho_{SWCNT}}{\rho_M}\right) - \left(\frac{\rho_{SWCNT}}{\rho_M}\right) w_{SWCNT}} \quad (2)$$

In Eq. (2), ρ_{SWCNT} , ρ_M and w_{SWCNT} are the modulus of elasticity of the single-walled carbon nanotube, polymeric matrix of composite nano-platelets and the mass fraction of the single-walled carbon nanotube, respectively (Shen 2009).

2.3 Extended blending law

In the developed mixing method, the properties of composite facing materials using the following equations are determined (Alibeigloo 2014)

$$\begin{aligned} E_1 &= \eta_1 E_{11} V_{SWCNT} + E_m V_m \\ \frac{\eta_2}{E_2} &= \frac{V_{SWCNT}}{E_{22}} + \frac{V_m}{E_m} \\ \frac{\eta_3}{G_2} &= \frac{V_{SWCNT}}{G_{12}} + \frac{V_m}{G_m} \end{aligned} \quad (3)$$

where, η_1 , η_2 and η_3 are constants by comparison with molecular dynamics simulations determined and usually are between zero and one variable. E_{11} , E_{22} and G_{12} are the longitudinal, transverse and shear modulus of the nanotube, respectively.

2.4 Sandwich kinematics

The sandwich plate from three layers, top, center and bottom composed. The displacements fields in face sheets, $u_i(x,y,z,t)$, $v_i(x,y,z,t)$ and $w_i(x,y,z,t)$ in the direction of x , y and z , respectively as follows are explained (Reddy 2003).

$$\begin{aligned} u(x,y,z,t) &= u_{0i}(x,y,t) + zu_{1i}(x,y,t) + z^2u_{2i}(x,y,t) + z^3u_{3i}(x,y,t) \\ v(x,y,z,t) &= v_{0i}(x,y,t) + zv_{1i}(x,y,t) + z^2v_{2i}(x,y,t) + z^3v_{3i}(x,y,t) \\ w(x,y,z,t) &= w_{0i}(x,y,t) + zw_{1i}(x,y,t) + z^2w_{2i}(x,y,t) \end{aligned} \quad (4)$$

The displacements fields for center layer are derived as Khalili and Mohammadi (2012)

$$\begin{aligned} u(x,y,z,t) &= u_{0c}(x,y,t) + zu_{1c}(x,y,t) + z^2u_{2c}(x,y,t) + z^3u_{3c}(x,y,t) \\ v(x,y,z,t) &= v_{0c}(x,y,t) + zv_{1c}(x,y,t) + z^2v_{2c}(x,y,t) + z^3v_{3c}(x,y,t) \\ w(x,y,z,t) &= w_{0c}(x,y,t) + zw_{1c}(x,y,t) + z^2w_{2c}(x,y,t) \end{aligned} \quad (5)$$

2.5 The stress-strain relations and stress resultants

The stress-strain relations for the top and bottom layers made of piezoelectric composite materials are as

$$\begin{aligned} \begin{Bmatrix} \sigma_{xx}^p \\ \sigma_{yy}^p \\ \sigma_{zz}^p \\ \sigma_{yz}^p \\ \sigma_{xz}^p \\ \sigma_{xy}^p \end{Bmatrix} &= \begin{bmatrix} Q_{11}^p & Q_{12}^p & Q_{13}^p & 0 & 0 & Q_{16}^p \\ Q_{12}^p & Q_{22}^p & Q_{23}^p & 0 & 0 & Q_{26}^p \\ Q_{13}^p & Q_{23}^p & Q_{33}^p & 0 & 0 & 0 \\ 0 & 0 & 0 & Q_{44}^p & 0 & 0 \\ 0 & 0 & 0 & 0 & Q_{55}^p & 0 \\ Q_{16}^p & Q_{26}^p & 0 & 0 & 0 & Q_{66}^p \end{bmatrix} \begin{Bmatrix} \varepsilon_x^p - \delta_{11}^p \Delta T - \chi_{11}^p \Delta H \\ \varepsilon_y^p - \delta_{22}^p \Delta T - \chi_{22}^p \Delta H \\ \varepsilon_z^p - \delta_{33}^p \Delta T - \chi_{33}^p \Delta H \\ \gamma_{yz}^p \\ \gamma_{xz}^p \\ \gamma_{xy}^p \end{Bmatrix} - \begin{bmatrix} 0 & 0 & e_{31}^p \\ 0 & 0 & e_{32}^p \\ 0 & 0 & e_{33}^p \\ 0 & e_{24}^p & 0 \\ e_{15}^p & 0 & 0 \\ 0 & 0 & 0 \end{bmatrix} \begin{Bmatrix} E_x^p \\ E_y^p \\ E_z^p \end{Bmatrix} \\ \\ \begin{Bmatrix} D_x^p \\ D_y^p \\ D_z^p \end{Bmatrix} &= \begin{bmatrix} 0 & 0 & 0 & e_{15}^p & 0 & 0 \\ 0 & 0 & e_{24}^p & 0 & 0 & 0 \\ e_{31}^p & e_{32}^p & e_{33}^p & 0 & 0 & 0 \end{bmatrix} \begin{Bmatrix} \varepsilon_x^p \\ \varepsilon_y^p \\ \varepsilon_z^p \\ \gamma_{yz}^p \\ \gamma_{xz}^p \\ \gamma_{xy}^p \end{Bmatrix} + \begin{bmatrix} \zeta_{11}^p & 0 & 0 \\ 0 & \zeta_{22}^p & 0 \\ 0 & 0 & \zeta_{33}^p \end{bmatrix} \begin{Bmatrix} E_x^p \\ E_y^p \\ E_z^p \end{Bmatrix} \quad p = t, b \end{aligned} \quad (6)$$

where Q_{ij}^p , e_{ij}^p , ζ_{ii}^p , δ_{ii}^p and χ_{ii}^p are the coefficients of rigidity, piezoelectric, dielectric, thermal expansion and moisture, respectively. The components of stress, normal strain, shear strain, electric displacement, electric field, temperature and humidity changes with σ_{ij}^p , ε_{ii}^p , γ_{ij}^p , D_i^p , E_i^p , ΔT and ΔH are exposed, respectively. An electric field is written as follows in terms of electric potential function

$$(E_x, E_y, E_z) = (\phi_{,x}, \phi_{,y}, \phi_{,z}) \quad (7)$$

where

$$\phi(x,y,z) = -\cos(\pi z/h) \phi(x,y) + zV_0 e^{i\omega t} / 2h \quad (8)$$

where V_0 , $\phi(x,y)$ and ω are direct voltage, two-dimensional electric potential function and natural frequency, respectively. Using the Eqs. (6)-(8), the strains for the three layers of sandwich structures

are obtained as follows

$$\begin{aligned}
\varepsilon_x^p &= \frac{\partial u_p}{\partial x} = \frac{\partial u_{0p}}{\partial x} + z \frac{\partial u_{1p}}{\partial x} + z^2 \frac{\partial u_{2p}}{\partial x} + z^3 \frac{\partial u_{3p}}{\partial x} + \frac{1}{2} \left(\frac{\partial w_{0p}}{\partial x} \right)^2 \\
\varepsilon_y^p &= \frac{\partial v_p}{\partial y} = \frac{\partial v_{0p}}{\partial y} + z \frac{\partial v_{1p}}{\partial y} + z^2 \frac{\partial v_{2p}}{\partial y} + z^3 \frac{\partial v_{3p}}{\partial y} + \frac{1}{2} \left(\frac{\partial w_{0p}}{\partial y} \right)^2 \\
\varepsilon_z^p &= \frac{\partial w_p}{\partial z} = w_1(x, y, t) + 2zw_2(x, y, t) \\
\gamma_{xy}^p &= \frac{\partial u_p}{\partial y} + \frac{\partial v_p}{\partial x} = \frac{\partial u_{0p}}{\partial y} + \frac{\partial v_{0p}}{\partial x} + z \frac{\partial u_{1p}}{\partial y} + z \frac{\partial v_{1p}}{\partial x} + z^2 \frac{\partial u_{2p}}{\partial y} + z^2 \frac{\partial v_{2p}}{\partial x} + z^3 \frac{\partial u_{3p}}{\partial y} \\
&\quad + z^3 \frac{\partial v_{3p}}{\partial x} + \frac{1}{2} \frac{\partial w_{0p}}{\partial y} \frac{\partial w_{0p}}{\partial x} \\
\gamma_{yz}^p &= \frac{\partial w_p}{\partial y} + \frac{\partial v_p}{\partial z} = \frac{\partial w_{0p}}{\partial y} + z \frac{\partial w_{1p}}{\partial y} + z^2 \frac{\partial w_{2p}}{\partial y} + v_{1p} + 2zv_{2p} + 3z^2v_{3p} \\
\gamma_{xz}^p &= \frac{\partial w_p}{\partial x} + \frac{\partial u_p}{\partial z} = \frac{\partial w_{0p}}{\partial x} + z \frac{\partial w_{1p}}{\partial x} + z^2 \frac{\partial w_{2p}}{\partial x} + u_{1p} + 2zu_{2p} + 3z^2u_{3p}
\end{aligned} \quad (9)$$

The stress-strain relationships for the center layer made of isotropic materials are as follows (Khalili *et al.* 2012)

$$\begin{Bmatrix} \sigma_x \\ \sigma_y \\ \sigma_z \\ \sigma_{yz} \\ \sigma_{xz} \\ \sigma_{xy} \end{Bmatrix} = \begin{bmatrix} Q_{11}^c & Q_{12}^c & Q_{13}^c & 0 & 0 & 0 \\ Q_{12}^c & Q_{22}^c & Q_{23}^c & 0 & 0 & 0 \\ Q_{13}^c & Q_{23}^c & Q_{33}^c & 0 & 0 & 0 \\ 0 & 0 & 0 & Q_{44}^c & 0 & 0 \\ 0 & 0 & 0 & 0 & Q_{55}^c & 0 \\ 0 & 0 & 0 & 0 & 0 & Q_{66}^c \end{bmatrix} \begin{Bmatrix} \varepsilon_x^c - \delta_{11}^c \Delta T - \chi_{11}^c \Delta H \\ \varepsilon_y^c - \delta_{22}^c \Delta T - \chi_{22}^c \Delta H \\ \varepsilon_z^c - \delta_{33}^c \Delta T - \chi_{33}^c \Delta H \\ \gamma_{yz}^c \\ \gamma_{xz}^c \\ \gamma_{xy}^c \end{Bmatrix} \quad (10)$$

The values of stiffness coefficients (Q) in Eq. (10) are as follows

$$\begin{aligned}
Q_{11}^c &= Q_{22}^c = Q_{33}^c = 2\mu + \lambda = \frac{E_c}{(1 + \nu_c)} + \frac{\nu E_c}{(1 + \nu_c)(1 - 2\nu_c)} \\
Q_{12}^c &= Q_{13}^c = Q_{23}^c = \frac{\nu E_c}{(1 + \nu_c)(1 - 2\nu_c)} \\
Q_{44}^c &= Q_{55}^c = Q_{66}^c = \mu = \frac{E_c}{2(1 + \nu_c)}
\end{aligned} \quad (11)$$

Based on the relations of strain potential energy, the stress resultants in the face-sheets and core are calculated as follows.

$$\begin{Bmatrix} N_x^p \\ N_y^p \\ N_z^p \\ N_{xy}^p \\ N_{yz}^p \\ N_{xz}^p \end{Bmatrix} = \int_{-\frac{h_p}{2}}^{\frac{h_p}{2}} \begin{Bmatrix} \sigma_{xx}^p \\ \sigma_{yy}^p \\ \sigma_{zz}^p \\ \sigma_{xy}^p \\ \sigma_{yz}^p \\ \sigma_{xz}^p \end{Bmatrix} dz, \quad \begin{Bmatrix} M_x^p \\ M_y^p \\ M_z^p \\ M_{xy}^p \\ M_{yz}^p \\ M_{xz}^p \end{Bmatrix} = \int_{-\frac{h_p}{2}}^{\frac{h_p}{2}} \begin{Bmatrix} \sigma_{xx}^p \\ \sigma_{yy}^p \\ \sigma_{zz}^p \\ \sigma_{xy}^p \\ \sigma_{yz}^p \\ \sigma_{xz}^p \end{Bmatrix} z dz \quad (12)$$

$$\begin{aligned} \begin{pmatrix} P_x^p \\ P_y^p \\ P_{xy}^p \end{pmatrix} &= \int_{-h_p/2}^{-h_p/2} \begin{pmatrix} \sigma_{xx}^p \\ \sigma_{yy}^p \\ \sigma_{xy}^p \end{pmatrix} z^2 dz, & \begin{pmatrix} R_x^p \\ R_y^p \\ R_{xy}^p \end{pmatrix} &= \int_{-h_p/2}^{-h_p/2} \begin{pmatrix} \sigma_{xx}^p \\ \sigma_{yy}^p \\ \sigma_{xy}^p \end{pmatrix} z^3 dz \\ \begin{pmatrix} R_{yz}^p \\ R_{xz}^p \end{pmatrix} &= \int_{-h_p/2}^{-h_p/2} \begin{pmatrix} \sigma_{yz}^p \\ \sigma_{xz}^p \end{pmatrix} z^2 dz, & p &= t, c, b \end{aligned} \quad (12)$$

After simplifying the relationships, the values obtained for the stress results in Eq. (12) are as Appendix A.

3. Governing equations

The governing equations of motion for the face sheets and the core using Hamilton's principle are derived.

$$\begin{aligned} \int \delta \Pi_p dt &= \int (\delta \Pi_t + \delta \Pi_c + \delta \Pi_b) dt = 0 \\ \int [(\delta T_t + \delta T_c + \delta T_b) - (\delta W_{ext}^t + \delta U_t + \delta W_{ext}^c + \delta U_c + \delta W_{ext}^b + \delta U_b + \delta C)] dt &= 0 \end{aligned} \quad (13)$$

where $\delta \Pi_t$, $\delta \Pi_c$ and $\delta \Pi_b$ are potential energies, top face, center, bottom face in the sandwich structures, respectively. δT_t , δU_t , δW_{ext}^t , δT_c , δU_c , δW_{ext}^c , δT_b , δU_b and δW_{ext}^b are kinetic energy, the strain energy, the work done by external forces for the upper, central, lower faces and δ denotes the variation operator. δC is the boundary conditions related to displacements, strains and stresses. Also, the external forces for the sandwich structure in Eq. (13) are the Lorentz forces due to the magnetic field, the compressive forces and the viscoelastic foundation forces. p is the apparent index represents the sandwich structure faces, for the top face $p = t$, for the center face (core) $p = c$ and bottom face $p = b$.

The variation of kinetic energy is extracted as follows.

$$\begin{aligned} \delta T &= \sum_{p=t,c,b} \int_V \rho \left[\begin{aligned} & - \left(\frac{\partial^2 u_{0p}}{\partial t^2} + z \frac{\partial^2 u_{1p}}{\partial t^2} + z^2 \frac{\partial^2 u_{2p}}{\partial t^2} + z^3 \frac{\partial^2 u_{3p}}{\partial t^2} \right) \delta u_{0p} - \left(z \frac{\partial^2 u_{0p}}{\partial t^2} + z^2 \frac{\partial^2 u_{1p}}{\partial t^2} \right. \\ & + z^3 \frac{\partial^2 u_{2p}}{\partial t^2} + z^4 \frac{\partial^2 u_{3p}}{\partial t^2} \left. \right) \delta u_{1p} - \left(z^2 \frac{\partial^2 u_{0p}}{\partial t^2} + z^3 \frac{\partial^2 u_{1p}}{\partial t^2} + z^4 \frac{\partial^2 u_{2p}}{\partial t^2} + z^5 \frac{\partial^2 u_{3p}}{\partial t^2} \right) \\ & \delta u_{2p} - \left(z^3 \frac{\partial^2 u_{0p}}{\partial t^2} + z^4 \frac{\partial^2 u_{1p}}{\partial t^2} + z^5 \frac{\partial^2 u_{2p}}{\partial t^2} + z^6 \frac{\partial^2 u_{3p}}{\partial t^2} \right) \delta u_{3p} - \left(\frac{\partial^2 v_{0p}}{\partial t^2} + z \frac{\partial^2 v_{1p}}{\partial t^2} \right. \\ & + z^2 \frac{\partial^2 v_{2p}}{\partial t^2} + z^3 \frac{\partial^2 v_{3p}}{\partial t^2} \left. \right) \delta v_{0p} - \left(z \frac{\partial^2 v_{0p}}{\partial t^2} + z^2 \frac{\partial^2 v_{1p}}{\partial t^2} + z^3 \frac{\partial^2 v_{2p}}{\partial t^2} + z^4 \frac{\partial^2 v_{3p}}{\partial t^2} \right) \\ & \delta v_{1p} - \left(z^2 \frac{\partial^2 v_{0p}}{\partial t^2} + z^3 \frac{\partial^2 v_{1p}}{\partial t^2} + z^4 \frac{\partial^2 v_{2p}}{\partial t^2} + z^5 \frac{\partial^2 v_{3p}}{\partial t^2} \right) \delta v_{2p} - \left(z^3 \frac{\partial^2 v_{0p}}{\partial t^2} + z^4 \frac{\partial^2 v_{1p}}{\partial t^2} \right. \\ & + z^5 \frac{\partial^2 v_{2p}}{\partial t^2} + z^6 \frac{\partial^2 v_{3p}}{\partial t^2} \left. \right) \delta v_{3p} - \left(\frac{\partial^2 w_{0p}}{\partial t^2} + z \frac{\partial^2 w_{1p}}{\partial t^2} + z^2 \frac{\partial^2 w_{2p}}{\partial t^2} \right) \delta w_{0p} - \left(z \frac{\partial^2 w_{0p}}{\partial t^2} \right. \\ & + z^2 \frac{\partial^2 w_{1p}}{\partial t^2} + z^3 \frac{\partial^2 w_{2p}}{\partial t^2} \left. \right) \delta w_{1p} - \left(z^2 \frac{\partial^2 w_{0p}}{\partial t^2} + z^3 \frac{\partial^2 w_{1p}}{\partial t^2} + z^4 \frac{\partial^2 w_{2p}}{\partial t^2} \right) \delta w_{2p} \end{aligned} \right] dV \quad (14) \end{aligned}$$

The following boundary conditions by applying the changes to the Eq. (14) are obtained.

$$\delta T_{b,c} = \sum_{p=t,c,b} \int_V \rho \left[\begin{aligned} & \left[\left(\frac{\partial u_{0p}}{\partial t} + z \frac{\partial u_{1p}}{\partial t} + z^2 \frac{\partial u_{2p}}{\partial t} + z^3 \frac{\partial u_{3p}}{\partial t} \right) \delta u_{0p} \right]_0^t + \left[\left(z \frac{\partial u_{0p}}{\partial t} + z^2 \frac{\partial u_{1p}}{\partial t} + z^3 \frac{\partial u_{2p}}{\partial t} \right. \right. \\ & \left. \left. + z^4 \frac{\partial u_{3p}}{\partial t} \right) \delta u_{1p} \right]_0^t + \left[\left(z^2 \frac{\partial u_{0p}}{\partial t} + z^3 \frac{\partial u_{1p}}{\partial t} + z^4 \frac{\partial u_{2p}}{\partial t} + z^5 \frac{\partial u_{3p}}{\partial t} \right) \delta u_{2p} \right]_0^t + \left[\left(z^3 \frac{\partial u_{0p}}{\partial t} \right. \right. \\ & \left. \left. + z^4 \frac{\partial u_{1p}}{\partial t} + z^5 \frac{\partial u_{2p}}{\partial t} + z^6 \frac{\partial u_{3p}}{\partial t} \right) \delta u_{3p} \right]_0^t + \left[\left(\frac{\partial v_{0p}}{\partial t} + z \frac{\partial v_{1p}}{\partial t} + z^2 \frac{\partial v_{2p}}{\partial t} + z^3 \frac{\partial v_{3p}}{\partial t} \right) \right. \\ & \left. \delta v_{0p} \right]_0^t + \left[\left(z \frac{\partial v_{0p}}{\partial t} + z^2 \frac{\partial v_{1p}}{\partial t} + z^3 \frac{\partial v_{2p}}{\partial t} + z^4 \frac{\partial v_{3p}}{\partial t} \right) \delta v_{1p} \right]_0^t + \left[\left(z^2 \frac{\partial v_{0p}}{\partial t} + z^3 \frac{\partial v_{1p}}{\partial t} + \right. \right. \\ & \left. \left. + z^4 \frac{\partial v_{2p}}{\partial t} + z^5 \frac{\partial v_{3p}}{\partial t} \right) \delta v_{2p} \right]_0^t + \left[\left(z^3 \frac{\partial v_{0p}}{\partial t} + z^4 \frac{\partial v_{1p}}{\partial t} + z^5 \frac{\partial v_{2p}}{\partial t} + z^6 \frac{\partial v_{3p}}{\partial t} \right) \delta v_{3p} \right]_0^t \\ & \left. + \left[\left(\frac{\partial w_{0p}}{\partial t} + z \frac{\partial w_{1p}}{\partial t} + z^2 \frac{\partial w_{2p}}{\partial t} \right) \delta w_{0p} \right]_0^t + \left[\left(z \frac{\partial w_{0p}}{\partial t} + z^2 \frac{\partial w_{1p}}{\partial t} + z^3 \frac{\partial w_{2p}}{\partial t} \right) \delta w_{1p} \right]_0^t \right. \\ & \left. + \left[\left(z^2 \frac{\partial w_{0p}}{\partial t} + z^3 \frac{\partial w_{1p}}{\partial t} + z^4 \frac{\partial w_{2p}}{\partial t} \right) \delta w_{2p} \right]_0^t \right] dV \quad (15) \end{aligned}$$

The variation of strain energy can be written as below.

$$\begin{aligned} \delta U &= \sum_{p=t,c,b} \int_V \left(\sigma_{xx}^p \delta \varepsilon_x^p + \sigma_{yy}^p \delta \varepsilon_y^p + \sigma_{zz}^p \delta \varepsilon_z^p + \sigma_{xy}^p \delta \gamma_{xy}^p + \sigma_{yz}^p \delta \gamma_{yz}^p + \sigma_{xz}^p \delta \gamma_{xz}^p \right) dV \\ &= \sum_{p=t,c,b} \int_V \left(+D_x^p \delta E_{,x}^p + D_y^p \delta E_{,y}^p + D_z^p \delta E_{,z}^p \right) dV \quad (16) \\ &= \sum_{p=t,c,b} \int_V \left(\sigma_{xx}^p \delta \varepsilon_x^p + \sigma_{yy}^p \delta \varepsilon_y^p + \sigma_{zz}^p \delta \varepsilon_z^p + \sigma_{xy}^p \delta \gamma_{xy}^p + \sigma_{yz}^p \delta \gamma_{yz}^p + \sigma_{xz}^p \delta \gamma_{xz}^p \right) dV \\ &= \sum_{p=t,c,b} \int_V \left(+D_x^p \delta \phi_{,x}^p + D_y^p \delta \phi_{,y}^p + D_z^p \delta \phi_{,z}^p \right) dV \end{aligned}$$

With some algebraic manipulation and simplifying are obtained.

$$\delta U = \sum_{p=t,c,b} \int_V \left(\begin{aligned} & \sigma_{xx}^p \left[\frac{\partial \delta u_{0p}}{\partial x} + z \frac{\partial \delta u_{1p}}{\partial x} + z^2 \frac{\partial \delta u_{2p}}{\partial x} + z^3 \frac{\partial \delta u_{3p}}{\partial x} \right] + \\ & \sigma_{yy}^p \left[\frac{\partial \delta v_{0p}}{\partial y} + z \frac{\partial \delta v_{1p}}{\partial y} + z^2 \frac{\partial \delta v_{2p}}{\partial y} + z^3 \frac{\partial \delta v_{3p}}{\partial y} \right] + \sigma_{zz}^p \left[\delta w_{1p} + 2z \delta w_{2p} \right] + \\ & \sigma_{xy}^p \left[\frac{\partial \delta u_{0p}}{\partial y} + \frac{\partial \delta v_{0p}}{\partial x} + z \frac{\partial \delta u_{1p}}{\partial y} + z \frac{\partial \delta v_{1p}}{\partial x} + z^2 \frac{\partial \delta u_{2p}}{\partial y} + \right. \\ & \left. z^2 \frac{\partial \delta v_{2p}}{\partial x} + z^3 \frac{\partial \delta u_{3p}}{\partial y} + z^3 \frac{\partial \delta v_{3p}}{\partial x} \right] + \\ & \sigma_{yz}^p \left[\frac{\partial \delta w_{0p}}{\partial y} + z \frac{\partial \delta w_{1p}}{\partial y} + z^2 \frac{\partial \delta w_{2p}}{\partial y} + \delta v_{1p} + \right. \\ & \left. 2z \delta v_{2p} + 3z^2 \delta v_{3p} \right] + \\ & \sigma_{xz}^p \left[\frac{\partial \delta w_{0p}}{\partial x} + z \frac{\partial \delta w_{1p}}{\partial x} + z^2 \frac{\partial \delta w_{2p}}{\partial x} + \delta u_{1p} + 2z \delta u_{2p} + 3z^2 \delta u_{3p} \right] + \\ & D_x^p \delta \phi_{,x}^p + D_y^p \delta \phi_{,y}^p + D_z^p \delta \phi_{,z}^p \end{aligned} \right) dV \quad (17)$$

The following boundary conditions for the Eq. (16) are obtained.

$$\delta U_{b,c} = \sum_{p=t,c,b} \int_V \left(\begin{aligned} & \left[(\sigma_{xx}^p \delta u_{0p})_{x_1}^{x_2} + (z \sigma_{xx}^p \delta u_{1p})_{x_1}^{x_2} + (z^2 \sigma_{xx}^p \delta u_{2p})_{x_1}^{x_2} + (z^3 \sigma_{xx}^p \delta u_{3p})_{x_1}^{x_2} \right] dz dy + \\ & \left[(\sigma_{yy}^p \delta v_{0p})_{y_1}^{y_2} + (z \sigma_{yy}^p \delta v_{1p})_{y_1}^{y_2} + (z^2 \sigma_{yy}^p \delta v_{2p})_{y_1}^{y_2} + (z^3 \sigma_{yy}^p \delta v_{3p})_{y_1}^{y_2} \right] dz dx + \\ & \left[(\sigma_{xy}^p \delta u_{0p})_{y_1}^{y_2} dz dx + (\sigma_{xy}^p \delta v_{0p})_{x_1}^{x_2} dz dy + (z \sigma_{xy}^p \delta u_{1p})_{y_1}^{y_2} dz dx + \right. \\ & \left. (z \sigma_{xy}^p \delta v_{1p})_{x_1}^{x_2} dz dy + (z^2 \sigma_{xy}^p \delta u_{2p})_{y_1}^{y_2} dz dx + (z^2 \sigma_{xy}^p \delta v_{2p})_{x_1}^{x_2} dz dy + \right. \\ & \left. (z^3 \sigma_{xy}^p \delta u_{3p})_{y_1}^{y_2} dz dx + (z^3 \sigma_{xy}^p \delta v_{3p})_{x_1}^{x_2} dz dy \right] + \\ & \left[(\sigma_{yz}^p \delta w_{0p})_{y_1}^{y_2} + (z \sigma_{yz}^p \delta w_{1p})_{y_1}^{y_2} + (z^2 \sigma_{yz}^p \delta w_{2p})_{y_1}^{y_2} \right] dz dx + \\ & \left[(\sigma_{xz}^p \delta w_{0p})_{x_1}^{x_2} + (z \sigma_{xz}^p \delta w_{1p})_{x_1}^{x_2} + (z^2 \sigma_{xz}^p \delta w_{2p})_{x_1}^{x_2} \right] dz dy \end{aligned} \right) \quad (18)$$

For further simplification of stresses and electrical displacement, are written the following as

$$\begin{aligned} \sigma_x^p &= Q_{11}^p \varepsilon_x^p + Q_{12}^p \varepsilon_y^p + Q_{13}^p \varepsilon_z^p + Q_{16}^p \gamma_{xy}^p + e_{31}^p \phi_{,z}^p \\ \sigma_y^p &= Q_{12}^p \varepsilon_x^p + Q_{22}^p \varepsilon_y^p + Q_{23}^p \varepsilon_z^p + Q_{26}^p \gamma_{xy}^p + e_{32}^p \phi_{,z}^p \\ \sigma_z^p &= Q_{13}^p \varepsilon_x^p + Q_{23}^p \varepsilon_y^p + Q_{33}^p \varepsilon_z^p + e_{33}^p \phi_{,z}^p \\ \sigma_{xy}^p &= Q_{44}^p \gamma_{xy}^p \\ \sigma_{yz}^p &= Q_{44}^p \gamma_{yz}^p + e_{24}^p \phi_{,y}^p \\ \sigma_{xz}^p &= Q_{44}^p \gamma_{xz}^p + e_{15}^p \phi_{,x}^p \\ D_x^p &= e_{15}^p \gamma_{xz}^p - \zeta_{11}^p \phi_{,x}^p \\ D_y^p &= e_{24}^p \gamma_{yz}^p - \zeta_{22}^p \phi_{,y}^p \\ D_z^p &= e_{31}^p \varepsilon_x^p + e_{32}^p \varepsilon_y^p + e_{33}^p \varepsilon_z^p - \zeta_{33}^p \phi_{,z}^p \\ p &= t, c, b \end{aligned} \quad (19)$$

Also in this study, in order to be precise the displacement field, the following conditions and constraints are considered:

- The equality of displacements at the boundary between the middle layer and the upper layer (participant equations λ_1, λ_3 and λ_5)
- The equality of displacements at the boundary between the middle layer and the lower layer (participant equations λ_2, λ_4 and λ_6)
- Zero transverse strain at free surface of upper layer (participant equations λ_7 and λ_8)
- Zero transverse strain at free surface of lower layer (participant equations λ_9 and λ_{10})
- The equalization of normal stress at the boundary between the middle layer and the upper layer (participant equations λ_{11})
- The equalization of normal stress at the boundary between the middle layer and the lower layer (participant equations λ_{12})
- The equality of transverse stresses at the boundary between the middle layer and the upper layer (participant equations λ_{13} and λ_{14})
- The equality of transverse stresses at the boundary between the middle layer and the lower layer (participant equations λ_{15} and λ_{16})

In this way, 16 new unknowns (λ_1 - λ_{16}) resulting from the conditions of displacements, strains and stresses at the common boundary of the layers are added to the 33 previous unknowns.

$$\delta c = \left[\begin{array}{l} \lambda_1 [u_t(x, y, h_t/2, t) - u_c(x, y, -h_c/2, t)] + \lambda_2 [u_b(x, y, -h_b/2, t) - u_c(x, y, h_c/2, t)] + \\ \lambda_3 [v_t(x, y, h_t/2, t) - v_c(x, y, -h_c/2, t)] + \lambda_4 [v_b(x, y, -h_b/2, t) - v_c(x, y, h_c/2, t)] + \\ \lambda_5 [w_t(x, y, h_t/2, t) - w_c(x, y, -h_c/2, t)] + \lambda_6 [w_b(x, y, -h_b/2, t) - w_c(x, y, h_c/2, t)] + \\ \lambda_7 [\gamma_{yz}^t(x, y, -h_t/2, t)] + \lambda_8 [\gamma_{xz}^t(x, y, -h_t/2, t)] + \lambda_9 [\gamma_{yz}^b(x, y, h_b/2, t)] + \lambda_{10} [\gamma_{xz}^b(x, y, h_b/2, t)] + \\ \int_V \delta \left[\begin{array}{l} Q_{31}^t \varepsilon_x^t(x, y, \frac{h_t}{2}, t) + Q_{32}^t \varepsilon_y^t(x, y, \frac{h_t}{2}, t) \\ + Q_{33}^t \varepsilon_z^t(x, y, \frac{h_t}{2}, t) + \\ \lambda_{11} \left[\begin{array}{l} Q_{36}^t \gamma_{yz}^t(x, y, \frac{h_t}{2}, t) - C_{31}^t \varepsilon_x^c(x, y, -\frac{h_c}{2}, t) \\ - C_{32}^t \varepsilon_y^c(x, y, -\frac{h_c}{2}, t) \\ - C_{33}^t \varepsilon_z^c(x, y, -\frac{h_c}{2}, t) \end{array} \right] + \lambda_{12} \left[\begin{array}{l} Q_{31}^b \varepsilon_x^b(x, y, -h_b/2, t) + Q_{32}^b \varepsilon_y^b(x, y, -h_b/2, t) + \\ Q_{33}^b \varepsilon_z^b(x, y, -h_b/2, t) + Q_{36}^b \gamma_{yz}^b(x, y, -h_b/2, t) - \\ C_{31}^t \varepsilon_x^c(x, y, h_c/2, t) - C_{32}^t \varepsilon_y^c(x, y, h_c/2, t) \\ - C_{33}^t \varepsilon_z^c(x, y, h_c/2, t) \end{array} \right] \end{array} \right] \\ + \lambda_{13} [Q_{44}^t \gamma_{yz}^t(x, y, h_t/2, t) - G_{yz}^c \gamma_{yz}^c(x, y, -h_c/2, t)] + \lambda_{14} [Q_{55}^t \gamma_{xz}^t(x, y, h_t/2, t) - G_{xz}^c \gamma_{xz}^c(x, y, -h_c/2, t)] + \\ \lambda_{15} [Q_{44}^b \gamma_{yz}^b(x, y, -h_b/2, t) - G_{yz}^c \gamma_{yz}^c(x, y, h_c/2, t)] + \lambda_{16} [Q_{55}^b \gamma_{xz}^b(x, y, -h_b/2, t) - G_{xz}^c \gamma_{xz}^c(x, y, h_c/2, t)] \end{array} \right] \quad (20)$$

The governing equations for a sandwich structure with viscoelastic piezoelectric composite face sheets reinforced by functionally graded carbon nanotubes (FG-CNTs) are derived. Hence, after integration by parts and some algebraic manipulation, thirty-three equations of motion are extracted, some of which are as follows:

At the top face sheet

$$\begin{aligned} \delta u_{1t}^t \frac{\partial^2 u_{0t}}{\partial t^2} + I_2^t \frac{\partial^2 u_{1t}}{\partial t^2} + I_3^t \frac{\partial^2 u_{2t}}{\partial t^2} + I_4^t \frac{\partial^2 u_{3t}}{\partial t^2} = -Q_1^t \frac{\partial^2 u_{0t}}{\partial x^2} - Q_2^t \frac{\partial^2 u_{1t}}{\partial x^2} - Q_3^t \frac{\partial^2 u_{2t}}{\partial x^2} - Q_4^t \frac{\partial^2 u_{3t}}{\partial x^2} - \\ Q_1^t \frac{\partial^2 v_{0t}}{\partial y \partial x} - Q_2^t \frac{\partial^2 v_{1t}}{\partial y \partial x} - Q_3^t \frac{\partial^2 v_{2t}}{\partial y \partial x} - Q_4^t \frac{\partial^2 v_{3t}}{\partial y \partial x} - 2Q_1^t u_{2t} - 6Q_2^t u_{3t} + B_{11}^t \frac{\partial^2 u_{0t}}{\partial x^2} + C_{11}^t \frac{\partial^2 u_{1t}}{\partial x^2} + \\ D_{11}^t \frac{\partial^2 u_{2t}}{\partial x^2} + E_{11}^t \frac{\partial^2 u_{3t}}{\partial x^2} + B_{12}^t \frac{\partial^2 v_{0t}}{\partial y \partial x} + C_{12}^t \frac{\partial v_{1t}^2}{\partial y \partial x} + D_{12}^t \frac{\partial v_{2t}}{\partial y} + E_{12}^t \frac{\partial v_{3t}}{\partial y} + B_{13}^p \frac{\partial w_1}{\partial x} + 2C_{13}^p \frac{\partial w_2}{\partial x} + \\ B_{16}^t \left(\frac{\partial^2 u_{0t}}{\partial y \partial x} + \frac{\partial^2 v_{0t}}{\partial x^2} \right) + C_{16}^t \left(\frac{\partial^2 u_{1t}}{\partial y \partial x} + \frac{\partial^2 v_{1t}}{\partial x^2} \right) + D_{16}^t \left(\frac{\partial^2 u_{2t}}{\partial y \partial x} + \frac{\partial^2 v_{2t}}{\partial x^2} \right) + E_{16}^t \left(\frac{\partial^2 u_{3t}}{\partial y \partial x} + \frac{\partial^2 v_{3t}}{\partial x^2} \right) \\ + Z_{312}^t \phi_{,x}^t + B_{66}^t \left(\frac{\partial^2 u_{0t}}{\partial y^2} + \frac{\partial^2 v_{0t}}{\partial x \partial y} \right) + C_{66}^t \left(\frac{\partial^2 u_{1t}}{\partial y^2} + \frac{\partial^2 v_{1t}}{\partial x \partial y} \right) + D_{66}^t \left(\frac{\partial^2 u_{2t}}{\partial y^2} + \frac{\partial^2 v_{2t}}{\partial x \partial y} \right) + E_{66}^t \left(\frac{\partial^2 u_{3t}}{\partial y^2} \right. \\ \left. + \frac{\partial^2 v_{3t}}{\partial x \partial y} \right) + A_{55}^t \frac{\partial w_{0t}}{\partial x} + B_{55}^t \frac{\partial w_{1t}}{\partial x} + C_{55}^t \frac{\partial w_{2t}}{\partial x} + A_{55}^t u_{1t} + 2B_{55}^t u_{2t} + 3C_{55}^t u_{3t} - Y_{15}^t \phi_{,x}^t(x, y, t) + \\ \frac{h_t}{2} \lambda_1 + \lambda_8 - \frac{\partial}{\partial x} (\lambda_{11} Q_{31}^t (h_t/2)) + \lambda_{14} Q_{55}^t = 0 \end{aligned} \quad (21)$$

$$\begin{aligned} \delta w_{0t}^t \frac{\partial^2 w_{0t}}{\partial t^2} + I_1^t \frac{\partial^2 w_{1t}}{\partial t^2} + I_2^t \frac{\partial^2 w_{2t}}{\partial t^2} = A_{44}^t \frac{\partial^2 w_{0t}}{\partial y^2} + B_{44}^t \frac{\partial^2 w_{1t}}{\partial y^2} + C_{44}^t \frac{\partial^2 w_{2t}}{\partial y^2} + A_{44}^t \frac{\partial v_{1t}}{\partial y} + 2B_{44}^t \frac{\partial v_{2t}}{\partial y} \\ + 3C_{44}^t \frac{\partial v_{3t}}{\partial y} - Y_{24}^t \phi_{,yy}^t(x, y, t) + A_{55}^t \frac{\partial w_{0t}}{\partial x^2} + B_{55}^t \frac{\partial w_{1t}}{\partial x^2} + C_{55}^t \frac{\partial^2 w_{2t}}{\partial x^2} + A_{55}^t \frac{\partial u_{1t}}{\partial x} + 2B_{55}^t \frac{\partial u_{2t}}{\partial x} + \\ 3C_{55}^t \frac{\partial u_{3t}}{\partial x} - Y_{15}^t \phi_{,xx}^t(x, y, t) + \lambda_5 - \frac{\partial}{\partial y} (\lambda_7) - \frac{\partial}{\partial x} (\lambda_8) - \frac{\partial}{\partial y} (\lambda_{11} Q_{36}^t) - \frac{\partial}{\partial y} (\lambda_{13} Q_{44}^t) - \frac{\partial}{\partial x} (\lambda_{14} Q_{55}^t) c_f \\ \frac{\partial w_{0t}}{\partial t} - \left[(N_{xt}^{cr} + N_{xt}^T + N_{xt}^H + 2e_{13} V_0) \frac{\partial^2 w_{0t}}{\partial x^2} + (N_{yt}^{cr} + N_{yt}^T + N_{yt}^H + 2e_{23} V_0) \frac{\partial^2 w_{0t}}{\partial y^2} \right] = 0 \end{aligned} \quad (22)$$

And at the core

$$\begin{aligned}
& \delta v_2^c I_2^c \frac{\partial^2 v_{0c}}{\partial t^2} + I_3^c \frac{\partial^2 v_{1c}}{\partial t^2} + I_4^c \frac{\partial^2 v_{2c}}{\partial t^2} + I_5^c \frac{\partial^2 v_{3c}}{\partial t^2} = -O_2^c \frac{\partial^2 v_{0c}}{\partial y^2} - O_3^c \frac{\partial^2 v_{1c}}{\partial y^2} - O_4^c \frac{\partial^2 v_{2c}}{\partial y^2} - O_5^c \frac{\partial^2 v_{3c}}{\partial y^2} \\
& - O_2^c \frac{\partial^2 u_{0c}}{\partial y \partial x} - O_3^c \frac{\partial^2 u_{1c}}{\partial y \partial x} - O_4^c \frac{\partial^2 u_{2c}}{\partial y \partial x} - O_5^c \frac{\partial^2 u_{3c}}{\partial y \partial x} - 2O_2^c v_{2c} - 6O_3^c v_{3c} + I_2^c \frac{\partial^2 v_{0c}}{\partial t^2} + I_3^c \frac{\partial^2 v_{1c}}{\partial t^2} + I_4^c \frac{\partial^2 v_{2c}}{\partial t^2} \\
& + I_5^c \frac{\partial^2 v_{3c}}{\partial t^2} = -O_2^c \frac{\partial^2 v_{0c}}{\partial y^2} - O_3^c \frac{\partial^2 v_{1c}}{\partial y^2} - O_4^c \frac{\partial^2 v_{2c}}{\partial y^2} - O_5^c \frac{\partial^2 v_{3c}}{\partial y^2} - O_2^c \frac{\partial^2 u_{0c}}{\partial y \partial x} - O_3^c \frac{\partial^2 u_{1c}}{\partial y \partial x} - O_4^c \frac{\partial^2 u_{2c}}{\partial y \partial x} \\
& - O_5^c \frac{\partial^2 u_{3c}}{\partial y \partial x} - 2O_2^c v_{2c} - 6O_3^c v_{3c} + C_{12}^c \frac{\partial u_{0c}}{\partial x \partial y} + D_{12}^c \frac{\partial^2 u_{1c}}{\partial x \partial y} + E_{12}^c \frac{\partial^2 u_{2c}}{\partial x \partial y} + F_{12}^c \frac{\partial^2 u_{3c}}{\partial x \partial y} + C_{22}^c \frac{\partial^2 v_{0c}}{\partial y^2} + \\
& D_{22}^c \frac{\partial^2 v_{1c}}{\partial y^2} + E_{22}^c \frac{\partial^2 v_{2c}}{\partial y^2} + F_{22}^c \frac{\partial^2 v_{3c}}{\partial y^2} + C_{23}^c \frac{\partial w_1}{\partial y} + 2D_{23}^c \frac{\partial w_2}{\partial y} + C_{26}^c \left(\frac{\partial^2 u_{0c}}{\partial y^2} + \frac{\partial^2 v_{0c}}{\partial x \partial y} \right) + D_{26}^c \left(\frac{\partial^2 u_{1c}}{\partial y^2} + \right. \\
& \left. \frac{\partial^2 v_{1c}}{\partial x \partial y} \right) + E_{26}^c \left(\frac{\partial^2 u_{2c}}{\partial y^2} + \frac{\partial^2 v_{2c}}{\partial x \partial y} \right) + F_{26}^c \left(\frac{\partial^2 u_{3c}}{\partial y^2} + \frac{\partial^2 v_{3c}}{\partial x \partial y} \right) + Z_{32zz}^c \phi_{,y} + C_{66}^c \left(\frac{\partial^2 u_{0c}}{\partial y \partial x} + \frac{\partial^2 v_{0c}}{\partial x^2} \right) + \\
& D_{66}^c \left(\frac{\partial^2 u_{1c}}{\partial y \partial x} + \frac{\partial^2 v_{1c}}{\partial x^2} \right) + E_{66}^c \left(\frac{\partial^2 u_{2c}}{\partial y \partial x} + \frac{\partial^2 v_{2c}}{\partial x^2} \right) + F_{66}^c \left(\frac{\partial^2 u_{3c}}{\partial y \partial x} + \frac{\partial^2 v_{3c}}{\partial x^2} \right) - 2B_{44}^c \frac{\partial w_{0c}}{\partial y} - 2C_{44}^c \frac{\partial w_{1c}}{\partial y} - \\
& 2D_{44}^c \frac{\partial w_{2c}}{\partial y} - 2B_{44}^c v_{1c} - 4C_{44}^c v_{2c} - 6D_{44}^c v_{3c} + 2Y_{24z}^c \phi_{,y} - \left(\frac{h_c}{2} \right)^2 \lambda_3 - \left(\frac{h_c}{2} \right)^2 \lambda_4 - \frac{\partial}{\partial y} (\lambda_{11} Q_{32}^c (h_c/2)^2) \\
& - \frac{\partial}{\partial x} (\lambda_{12} Q_{32}^c (h_c/2)^2) - h_c \lambda_{13} G_{yz}^c + h_c \lambda_{15} G_{yz}^c = 0
\end{aligned} \tag{23}$$

$$\begin{aligned}
& \delta w_0^c I_0^c \frac{\partial^2 w_{0c}}{\partial t^2} + I_1^c \frac{\partial^2 w_{1c}}{\partial t^2} + I_2^c \frac{\partial^2 w_{2c}}{\partial t^2} = A_{44}^c \frac{\partial^2 w_{0c}}{\partial y^2} + B_{44}^c \frac{\partial^2 w_{1c}}{\partial y^2} + C_{44}^c \frac{\partial^2 w_{2c}}{\partial y^2} + A_{44}^c \frac{\partial v_{1c}}{\partial y} \\
& 2B_{44}^c \frac{\partial v_{2c}}{\partial y} + 3C_{44}^c \frac{\partial v_{3c}}{\partial y} - Y_{24}^c \phi_{,yy} + A_{55}^c \frac{\partial^2 w_{0c}}{\partial x^2} + B_{55}^c \frac{\partial^2 w_{1c}}{\partial x^2} + C_{55}^c \frac{\partial^2 w_{2c}}{\partial x^2} + A_{55}^c \frac{\partial u_{1c}}{\partial x} + \\
& 2B_{55}^c \frac{\partial u_{2c}}{\partial x} + 3C_{55}^c \frac{\partial u_{3c}}{\partial x} - Y_{15}^c \phi_{,xx} + c_f \frac{\partial w_{0c}}{\partial t} - k_w w_{0c} + k_g \nabla^2 w_{0c} - c_f \frac{\partial w_{0c}}{\partial t} - \\
& \left[\left(N_{xc}^{cr} + N_{xc}^T + N_{xc}^H + 2e_{13} V_0 \right) \frac{\partial^2 w_{0c}}{\partial x^2} + \right. \\
& \left. \left(N_{yc}^{cr} + N_{yc}^T + N_{yc}^H + 2e_{23} V_0 \right) \frac{\partial^2 w_{0c}}{\partial y^2} \right] - \lambda_5 - \lambda_6 - \frac{\partial}{\partial y} (\lambda_{13} G_{yz}^c) - \frac{\partial}{\partial x} (\lambda_{14} G_{xz}^c) - \\
& \frac{\partial}{\partial y} (\lambda_{15} G_{yz}^c) - \frac{\partial}{\partial x} (\lambda_{16} G_{xz}^c) = 0
\end{aligned} \tag{24}$$

At the bottom face sheet

$$\begin{aligned}
& \delta u_0^b I_0^b \frac{\partial^2 u_{0b}}{\partial t^2} + I_1^b \frac{\partial^2 u_{1b}}{\partial t^2} + I_2^b \frac{\partial^2 u_{2b}}{\partial t^2} + I_3^b \frac{\partial^2 u_{3b}}{\partial t^2} = -O_0^b \frac{\partial^2 u_{0b}}{\partial x^2} - O_1^b \frac{\partial^2 u_{1b}}{\partial x^2} - O_2^b \frac{\partial^2 u_{2b}}{\partial x^2} - O_3^b \frac{\partial^2 u_{3b}}{\partial x^2} \\
& - O_0^b \frac{\partial^2 v_{0b}}{\partial y \partial x} - O_1^b \frac{\partial^2 v_{1b}}{\partial y \partial x} - O_2^b \frac{\partial^2 v_{2b}}{\partial y \partial x} - O_3^b \frac{\partial^2 v_{3b}}{\partial y \partial x} - 2O_0^b u_{2b} - 6O_1^b u_{3b} + A_{11}^b \frac{\partial^2 u_{0b}}{\partial x^2} + B_{11}^b \frac{\partial^2 u_{1b}}{\partial x^2} + \\
& C_{11}^b \frac{\partial^2 u_{2b}}{\partial x^2} + D_{11}^b \frac{\partial^2 u_{3b}}{\partial x^2} + A_{12}^b \frac{\partial^2 v_{0b}}{\partial y \partial x} + B_{12}^b \frac{\partial^2 v_{1b}}{\partial y \partial x} + C_{12}^b \frac{\partial^2 v_{2b}}{\partial y \partial x} + D_{12}^b \frac{\partial^2 v_{3b}}{\partial y \partial x} + A_{13}^b \frac{\partial w_1}{\partial x} + 2B_{13}^b \frac{\partial w_2}{\partial x} \\
& + A_{16}^b \left(\frac{\partial^2 u_{0b}}{\partial y \partial x} + \frac{\partial^2 v_{0b}}{\partial x^2} \right) + B_{16}^b \left(\frac{\partial^2 u_{1b}}{\partial y \partial x} + \frac{\partial^2 v_{1b}}{\partial x^2} \right) + C_{16}^b \left(\frac{\partial^2 u_{2b}}{\partial y \partial x} + \frac{\partial^2 v_{2b}}{\partial x^2} \right) + D_{16}^b \left(\frac{\partial^2 u_{3b}}{\partial y \partial x} + \frac{\partial^2 v_{3b}}{\partial x^2} \right) \\
& + Z_{31}^b \phi_{,x} + A_{66}^b \left(\frac{\partial^2 u_{0b}}{\partial y^2} + \frac{\partial^2 v_{0b}}{\partial x \partial y} \right) + B_{66}^b \left(\frac{\partial^2 u_{1b}}{\partial y^2} + \frac{\partial^2 v_{1b}}{\partial x \partial y} \right) + C_{66}^b \left(\frac{\partial^2 u_{2b}}{\partial y^2} + \frac{\partial^2 v_{2b}}{\partial x \partial y} \right) \\
& + D_{66}^b \left(\frac{\partial^2 u_{3b}}{\partial y^2} + \frac{\partial^2 v_{3b}}{\partial x \partial y} \right) + \lambda_2 - \frac{\partial}{\partial x} (\lambda_{12} Q_{31}^b) = 0
\end{aligned} \tag{25}$$

$$\begin{aligned}
& \delta v_2^b I_2^b \frac{\partial^2 v_{0b}}{\partial t^2} + I_3^b \frac{\partial^2 v_{1b}}{\partial t^2} + I_4^b \frac{\partial^2 v_{2b}}{\partial t^2} + I_5^b \frac{\partial^2 v_{3b}}{\partial t^2} = -O_2^b \frac{\partial^2 v_{0b}}{\partial y^2} - O_3^b \frac{\partial^2 v_{1b}}{\partial y^2} - O_4^b \frac{\partial^2 v_{2b}}{\partial y^2} - \\
& O_5^b \frac{\partial^2 v_{3b}}{\partial y^2} - O_2^b \frac{\partial^2 u_{0b}}{\partial y \partial x} - O_3^b \frac{\partial^2 u_{1b}}{\partial y \partial x} - O_4^b \frac{\partial^2 u_{2b}}{\partial y \partial x} - O_5^b \frac{\partial^2 u_{3b}}{\partial y \partial x} - 2O_2^b v_{2b} - 6O_3^b v_{3b} + \\
& C_{12}^b \frac{\partial^2 u_{0b}}{\partial x \partial y} + D_{12}^b \frac{\partial^2 u_{1b}}{\partial x \partial y} + E_{12}^b \frac{\partial^2 u_{2b}}{\partial x \partial y} + F_{12}^b \frac{\partial^2 u_{3b}}{\partial x \partial y} + C_{22}^b \frac{\partial^2 v_{0b}}{\partial y^2} + D_{22}^b \frac{\partial^2 v_{1b}}{\partial y^2} + E_{22}^b \frac{\partial^2 v_{2b}}{\partial y^2} + \\
& F_{22}^b \frac{\partial^2 v_{3b}}{\partial y^2} + C_{23}^b \frac{\partial w_1}{\partial y} + 2D_{23}^b \frac{\partial w_2}{\partial y} + C_{26}^b \left(\frac{\partial^2 u_{0b}}{\partial y^2} + \frac{\partial^2 v_{0b}}{\partial x \partial y} \right) + D_{26}^b \left(\frac{\partial^2 u_{1b}}{\partial y^2} + \frac{\partial^2 v_{1b}}{\partial x \partial y} \right) + \\
& E_{26}^b \left(\frac{\partial^2 u_{2b}}{\partial y^2} + \frac{\partial^2 v_{2b}}{\partial x \partial y} \right) + F_{26}^b \left(\frac{\partial^2 u_{3b}}{\partial y^2} + \frac{\partial^2 v_{3b}}{\partial x \partial y} \right) + Z_{32zz}^b \phi_{,y}^b + C_{66}^b \left(\frac{\partial^2 u_{0b}}{\partial y \partial x} + \frac{\partial^2 v_{0b}}{\partial x^2} \right) + \\
& D_{66}^b \left(\frac{\partial^2 u_{1b}}{\partial y \partial x} + \frac{\partial^2 v_{1b}}{\partial x^2} \right) + E_{66}^b \left(\frac{\partial^2 u_{2b}}{\partial y \partial x} + \frac{\partial^2 v_{2b}}{\partial x^2} \right) + F_{66}^b \left(\frac{\partial^2 u_{3b}}{\partial y \partial x} + \frac{\partial^2 v_{3b}}{\partial x^2} \right) - 2B_{44}^b \frac{\partial w_{0b}}{\partial y} - \\
& 2C_{44}^b \frac{\partial w_{1b}}{\partial y} - 2D_{44}^b \frac{\partial w_{2b}}{\partial y} - 2B_{44}^b v_{1b} - 4C_{44}^b v_{2b} - 6D_{44}^b v_{3b} + 2Y_{24z}^b \phi_{,y}^b + \left(\frac{h_b}{2} \right)^2 \lambda_4 + \\
& \lambda_9 - \frac{\partial}{\partial y} \left((h_b/2)^2 \lambda_{12} Q_{32}^b \right) - h_b \lambda_{12} Q_{36}^b - h_b \lambda_{15} Q_{44}^b = 0
\end{aligned} \tag{26}$$

And some from Lagrangian coefficients are as Appendix B.

4. Solution

In order to solve the free vibration problem of simply supported sandwich structure, the Navier method is applied (Qatu 2004). For satisfying the boundary conditions, the displacement fields based on double Fourier series are assumed to be in the following form

$$\begin{aligned}
u_{op}(x, y, t) &= \sum_{m=1}^{\infty} \sum_{n=1}^{\infty} u_{op}^{mn} e^{i\omega t} \sin\left(\frac{n\pi y}{b}\right) \cos\left(\frac{m\pi x}{a}\right) \\
u_{1p}(x, y, t) &= \sum_{m=1}^{\infty} \sum_{n=1}^{\infty} u_{1p}^{mn} e^{i\omega t} \sin\left(\frac{n\pi y}{b}\right) \cos\left(\frac{m\pi x}{a}\right) \\
u_{2p}(x, y, t) &= \sum_{m=1}^{\infty} \sum_{n=1}^{\infty} u_{2p}^{mn} e^{i\omega t} \sin\left(\frac{n\pi y}{b}\right) \cos\left(\frac{m\pi x}{a}\right) \\
u_{3p}(x, y, t) &= \sum_{m=1}^{\infty} \sum_{n=1}^{\infty} u_{3p}^{mn} e^{i\omega t} \sin\left(\frac{n\pi y}{b}\right) \cos\left(\frac{m\pi x}{a}\right) \\
v_{op}(x, y, t) &= \sum_{m=1}^{\infty} \sum_{n=1}^{\infty} v_{op}^{mn} e^{i\omega t} \cos\left(\frac{n\pi y}{b}\right) \sin\left(\frac{m\pi x}{a}\right) \\
v_{1p}(x, y, t) &= \sum_{m=1}^{\infty} \sum_{n=1}^{\infty} v_{1p}^{mn} e^{i\omega t} \cos\left(\frac{n\pi y}{b}\right) \sin\left(\frac{m\pi x}{a}\right) \\
v_{2p}(x, y, t) &= \sum_{m=1}^{\infty} \sum_{n=1}^{\infty} v_{2p}^{mn} e^{i\omega t} \cos\left(\frac{n\pi y}{b}\right) \sin\left(\frac{m\pi x}{a}\right)
\end{aligned} \tag{27}$$

$$\begin{aligned}
v_{3p}(x, y, t) &= \sum_{m=1}^{\infty} \sum_{n=1}^{\infty} v_{3p}^{mn} e^{i\omega t} \cos\left(\frac{n\pi y}{b}\right) \sin(m\pi x/a) \\
w_{op}(x, y, t) &= \sum_{m=1}^{\infty} \sum_{n=1}^{\infty} w_{op}^{mn} e^{i\omega t} \sin(n\pi y/b) \sin(m\pi x/a) \\
w_{1p}(x, y, t) &= \sum_{m=1}^{\infty} \sum_{n=1}^{\infty} w_{1p}^{mn} e^{i\omega t} \sin(n\pi y/b) \sin(m\pi x/a) \\
w_{2p}(x, y, t) &= \sum_{m=1}^{\infty} \sum_{n=1}^{\infty} w_{2p}^{mn} e^{i\omega t} \sin(n\pi y/b) \sin(m\pi x/a), \quad p = t, c, b \\
\phi^s(x, y, t) &= \sum_{m=1}^{\infty} \sum_{n=1}^{\infty} \phi^{smn} e^{i\omega t} \sin(n\pi y/b) \sin(m\pi x/a), \quad s = t, b
\end{aligned} \tag{27}$$

where m is the axial half-wave number and n is the circumferential wave number. Also, u_{0p}^{mn} , u_{1p}^{mn} , u_{2p}^{mn} , u_{3p}^{mn} , v_{op}^{mn} , v_{1p}^{mn} , v_{2p}^{mn} , v_{3p}^{mn} , w_{op}^{mn} , w_{1p}^{mn} , w_{2p}^{mn} , ϕ^{smn} are the constant amplitudes of vibrations associated with the natural mode shapes. Also, ω is the natural angular frequencies (rad/s) related to mode number (m, n).

And for the Lagrange coefficients are as Appendix C.

Then, above relationships are written in the following matrix

$$\begin{aligned}
M\ddot{Y} + C\dot{Y} + KY &= 0 \\
Y &= \begin{Bmatrix} u_{ip} \\ v_{ip} \\ w_{ip} \\ \phi^t \\ \phi^b \\ \lambda_j \end{Bmatrix}, \quad i = 1 - 33, \quad j = 1 - 16 \\
C &= c_s K + c_f
\end{aligned} \tag{28}$$

where c_s , c_f are structural damping coefficient and damping coefficient of viscoelastic foundation, respectively. Finally, by solving the Eq. (28) the natural frequency of the sandwich structure is calculated.

4. Numerical results and discussion

For validation, the present study with the analysis of vibration stability and bending of sandwich structures with composite faces based on higher order theory was compared. In this research, higher order theory with eleven degrees of freedom and a total of 33 degrees of freedom for sandwich structures was used. The present study deals with first-order shear deformation theory with five degrees of freedom (FSDT5), third-order shear deformation theory with seven degrees of freedom (TSDT7), and higher-order theories with nine, eleven, and thirteen degrees of freedom (HSDT) has been compared.

The properties of the materials used to validate the carbon nanotube-reinforced composite faces

Table 1 Properties of carbon nanotubes (Wang and Shen 2012)

$\alpha_{22} (\times 10^{-6}/\text{K})$	$\alpha_{11} (\times 10^{-6}/\text{K})$	$G_{12} (\text{TPa})$	$E_{11} (\text{TPa})$	$E_{11} (\text{TPa})$	T (K)
5.1682	3.4584	1.9445	7.0800	5.6466	300
5.0189	4.5381	1.9643	6.9348	5.5308	500
4.8943	4.6677	1.9644	6.8643	5.4744	700

Table 2 The properties of material for base (matrix) composite and core sandwich structure

$\alpha (\times 10^{-6}/\text{K})$	ν	$\rho (\text{kg}/\text{m}^3)$	E (GPa)	Material
$45(1 + 0.0000\Delta T)$	0.3	1150	(3.52-0.0034 T)	PMMA
$7.5788(1 + 6.638 \times 10^{-4}T - 3.147 \times 10^{-6} \times T^2)$	0.29	4429	$122.56(1 - 0.0004568T)$	Ti-6Al-4v

Table 3 The properties, matrix face of reinforced piezoelectric composite with single wall carbon nanotubes

Parameters	Polyvinylidene fluoride
E	8.3 GPa
ν	0.18
e_{31}	-0.13 C/m ²
e_{32}	-0.145 C/m ²
e_{15}	-0.009 C/m ²
e_{24}	-0.276 C/m ²

Table 4 The non-dimensional natural frequency of the square sandwich plate with reinforced composite faces and functional gradient nanotubes ($\Omega = \frac{\omega a^2}{h} \sqrt{\frac{\rho_c}{E_c}}$)

FSDT5 (Natarajan <i>et al.</i> 2014)	TSMT7 (Natarajan <i>et al.</i> 2014)	HSDT9 (Natarajan <i>et al.</i> 2014)	HSDT11B (Natarajan <i>et al.</i> 2014)	HSDT11A (Natarajan <i>et al.</i> 2014)	HSDT13 (Natarajan <i>et al.</i> 2014)	Present model	T(K)	Distribution nanotubes
4.2504	4.3199	4.1677	4.1736	3.8108	3.8203	4.2315	300	UD
4.0789	4.1501	3.9623	3.9680	3.5492	3.5588	4.0715	500	
4.4561	4.5394	4.2554	4.2602	3.7714	3.7815	3.1724	300	FG-X
4.2801	4.3657	4.0232	4.0277	3.4809	3.4910	3.9469	500	

and the isotropic core of the sandwich structure in the Tables 1-2 are shown.

The properties, matrix face of reinforced piezoelectric composite with single wall carbon nanotubes in the Table 3 was shown.

The non-dimensional natural frequency of the square sandwich plate ($\Omega = \frac{\omega a^2}{h} \sqrt{\frac{\rho_c}{E_c}}$) with reinforced composite faces and functional gradient nanotubes for different temperatures obtained the present study with the results of other researchers in Table 4 are presented (Pourmoayed *et al.* 2017). The ratio of length to thickness is five ($a/h = 5$), and the ratio of core thickness to face thickness is two ($h_c/h_f = 2$). The volume percentage of nanotubes is equal 0.17. There is a good agreement between the results of this study and the results of the theories expressed.

Based on the increase of volume percentages of fibers, the non-dimensional natural frequency

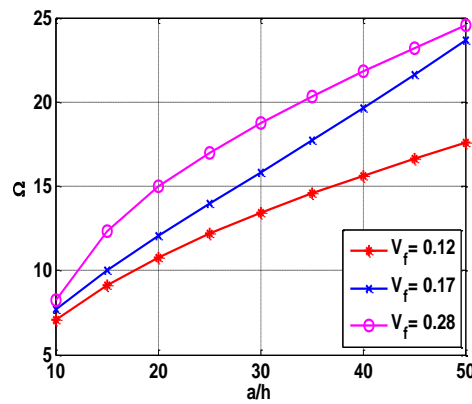


Fig. 2 Effect of a/h and volume percentages of fibers on non-dimensional frequency

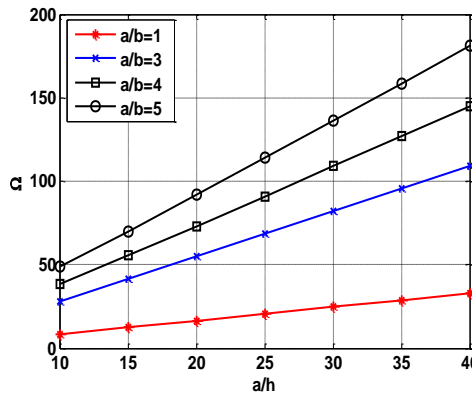


Fig. 3 The effect of the ratio of length-to-thickness (a/h) and length to width on non-dimensional frequency

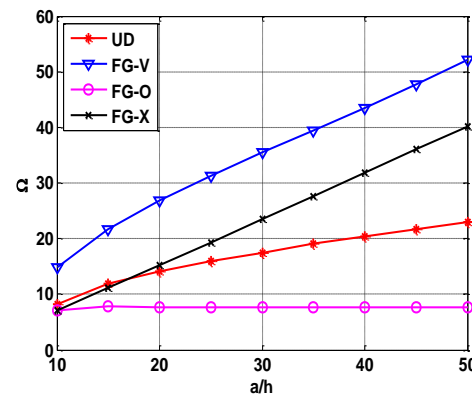


Fig. 4 The effect of different distributions of carbon nanotubes on non-dimensional natural frequency

increases (Fig. 2). Variation of non-dimensional natural frequency versus the ratio of length-to-thickness and length to width, shown in Fig. 3. It can be seen that by increasing the length-to-width ratio, the non-dimensional natural frequency increases.

The dimensionless natural frequency for the different distributions of carbon nanotubes in the

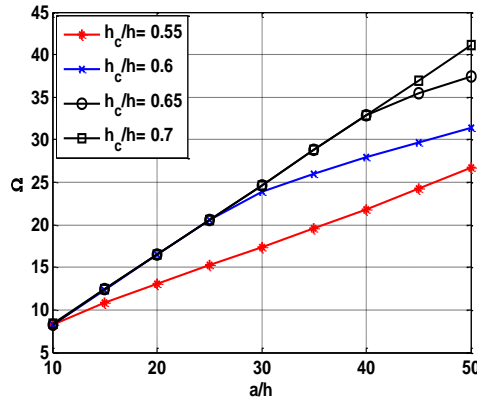


Fig. 5 Effect of core thickness on non-dimensional frequency of sandwich structures

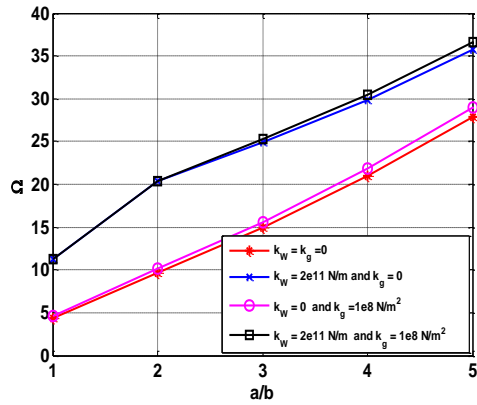


Fig. 6 The effect of elastic foundation on non-dimensional natural frequency of sandwich structures

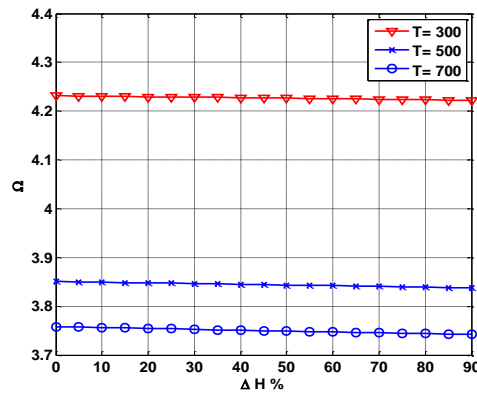


Fig. 7 The effect of temperature and humidity changes on the non-dimensional natural frequency of sandwich structures

upper and lower faces of the sandwich structure is shown in Fig. 4. These distributions include uniform shape (UD), O shape (FG-O), V shape (FG-V) and X shape (FG-X). According this shape,

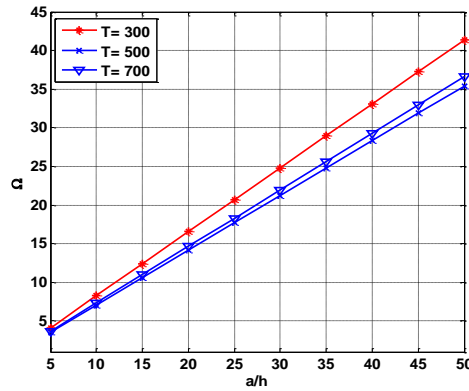


Fig. 8 The effect of different temperatures on the dimensionless natural frequency for different length to thickness ratios

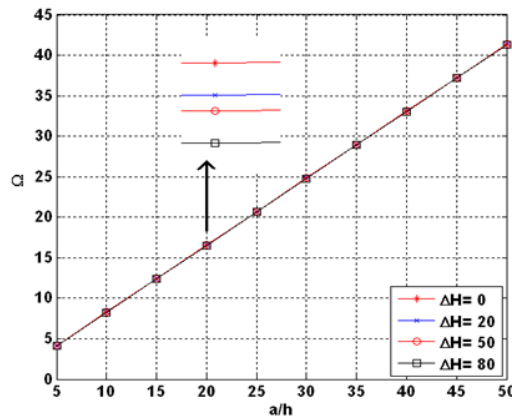


Fig. 9 The effect of moisture changes on non-dimensional natural frequency for different length to thickness ratios

the distribution of FG-V carbon nanotubes further strengthens the sandwich structure, resulting non-dimensional natural frequency has become more than other distributions.

The effect of core thickness on non-dimensional natural frequency can be seen in Fig. 5. Based on the increase in the ratio of core thickness to total thickness (h_c/h), the non-dimensional natural frequency increases. This incremental trend is important in the length-to-thickness ratios of this structure.

The influence of elastic foundation (Pasternak shear constant, k_g and Winkler spring constant, k_w) on the dimensionless natural frequency of sandwich structures in Fig. 6 is shown. As can be seen in this figure, with the elastic foundation, the structure becomes more rigid and its stiffness increases, resulting the dimensionless natural frequency of sandwich structures increase. Also, the effect of Winkler spring constant on the non-dimensional natural frequency is more than the effect of shear constant.

The effect of temperature changes and humidity changes on the non-dimensional natural frequency of sandwich structures is shown in Fig. 7. As shown in this figure, with increasing temperature and humidity changes, the structure becomes weaker and its stiffness decreases,

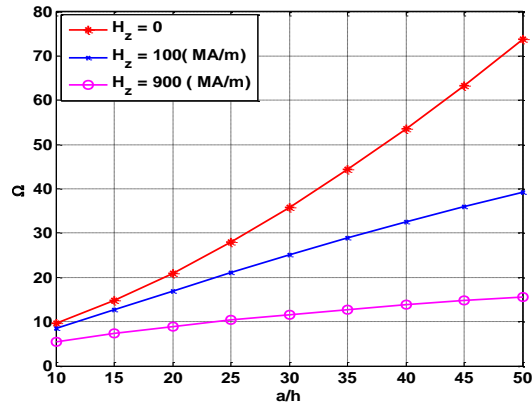


Fig. 10 The effect of magnetic field in along of thickness on non-dimensional natural frequency of sandwich structures

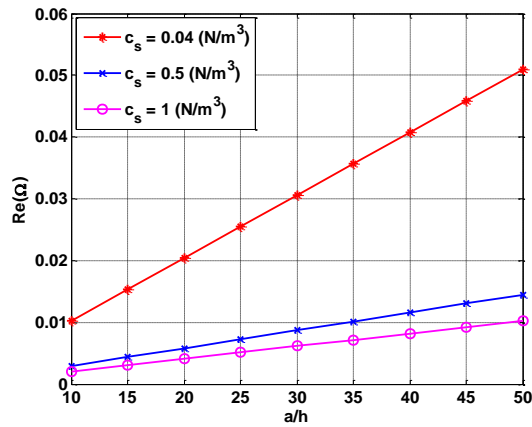


Fig. 11 The effect of viscosity of sandwich structure on real dimensionless natural frequency of sandwich structure

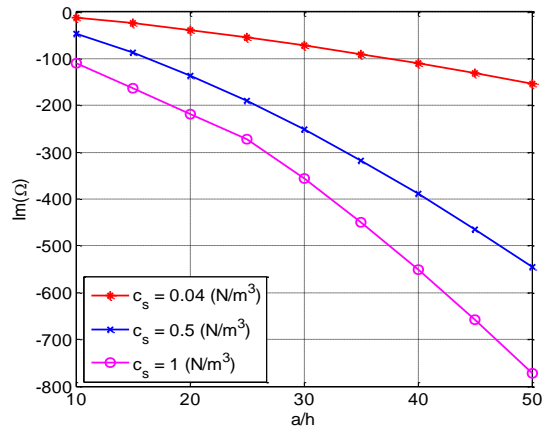


Fig. 12 The effect of viscosity of sandwich structure on imaginary dimensionless natural frequency of sandwich structure

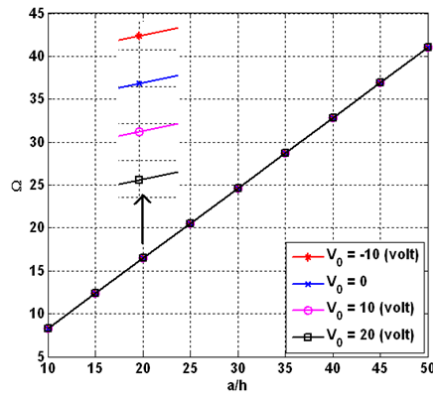


Fig. 13 The effect of applied voltage on non-dimensional natural frequency of sandwich structures

resulting non-dimensional natural frequency of sandwich structures has a decreasing trend for these changes. Also, the decreasing trend of the non-dimensional natural frequency of this structure with temperature changes is more than humidity changes.

The effect of different temperatures on the non-dimensional natural frequency of sandwich structures for different length-to-thickness ratios is shown in Fig. 8. As shown in this figure, by increasing the temperature from 300 to 700 degrees Kelvin, the dimensionless natural frequency of the sandwich structure decreases, and this trend of dimensionless natural frequency decreases in ratio length-to-thickness larger is important.

The effect of moisture changes on the dimensionless natural frequency of sandwich structures for different length-to-thickness ratios is shown in Fig. 9. As shown in this figure, with increasing of moisture ratio, the dimensionless natural frequency of the sandwich structure decreases.

The effect of the magnetic field in along thickness of the sandwich structure (H_z) on the non-dimensional natural frequency of the sandwich structure for different length to thickness ratios in Fig. 10 is shown. As it is shown in this figure, with increasing magnetic field, non-dimensional natural frequency of the sandwich structure decreases, because by applying this field, the pressure Lorentz forces create that cause decreases the flexibility of the structure and consequently non-dimensional natural frequency decreases.

The effect of the viscosity of the sandwich structure (c_s) on the real and imaginary dimensionless natural frequency of the sandwich structure for different length to thickness ratios is shown in Figs. 11-12. As can be seen in these figures, with increasing viscosity of sandwich structures, on real and imaginary dimensionless natural frequency of sandwich structure decrease.

The effect of applied voltage on the dimensionless natural frequency of sandwich structures for different length-to-thickness ratios is shown in Fig. 13. As shown in this figure, by applying negative voltage orientation the piezoelectric plate is such that it increases the dimensionless natural frequency. Contrary to negative voltage, applying positive voltage reduces the dimensionless natural frequency.

6. Conclusions

In this study, free vibration of sandwich structure with viscoelastic piezoelectric composite face

sheets reinforced by functionally graded carbon nanotubes was presented based on an improved higher-order sandwich panel theory. In order to be accurate, the displacement field is intended, based on compatibility conditions in the interface of the core and the top and bottom face sheets are considered. The nanotubes in the piezoelectric polymer composite faces have been distributed uniformly (*UD*), V-shaped (*FG-V*), O-shaped (*FG-O*) and X-shaped (*FG-X*). The governing equations of sandwich nano structure were obtained by Hamilton's principle and by Navier method of natural frequency for sandwich nano structures with simple support boundary conditions were calculated. The results of this study can be summarized as follows:

- The dimensionless natural frequency of sandwich nanostructures with increasing volume percent of single wall carbon nanotubes, a/b apparent coefficient, elastic foundation parameters, applied voltage increased.
- Increasing natural frequency of sandwich nano-structures with negative voltage applied more than positive voltage applied.
- Non dimensional natural frequency of sandwich nano-structures with increasing foundation, magnetic field and structure damping coefficients decreased.
- For different distributions of carbon single walled nanotubes in sandwich nanostructures, *FG-V* distribution and *FG-O* distribution have the largest and smallest dimensional natural frequencies.
- Non-dimensional natural frequency of sandwich structures with increasing temperature and humidity changes decreased.

References

- Akgöz, B. and Civalek, Ö. (2012), "Free vibration analysis for single-layered graphene sheets in an elastic matrix via modified couple stress theory", *Mater. Des.*, **42**, 164-171. <https://doi.org/10.1016/j.matdes.2012.06.002>.
- Alibeigloo, A. (2014), "Free vibration analysis of functionally graded carbon nanotube-reinforced composite cylindrical panel embedded in piezoelectric layers by using theory of elasticity", *Eur. J. Mech. A Solids.*, **44**, 104-115. <https://doi.org/10.1016/j.euromechsol.2013.10.002>.
- Asgari, G., Payganeh, G. and Malekzadeh Fard, K. (2019), "Dynamic instability and free vibration behavior of three-layered softcored sandwich beams on nonlinear elastic foundations", *Struct. Eng. Mech.*, **72**(4), 525-540. <https://doi.org/10.12989/sem.2019.72.4.525>.
- Bellifa, H., Benrahou, K.H., Hadji, L., Houari, M.S.A. and Tounsi, A. (2016), "Bending and free vibration analysis of functionally graded plates using a simple shear deformation theory and the concept the neutral surface position", *J. Braz. Soc. Mech. Sci. Eng.*, **38**(1), 265-275. <https://doi.org/10.1007/s40430-015-0354-0>.
- Bennoun, M., Houari, M.S.A. and Tounsi, A. (2016), "A novel five variable refined plate theory for vibration analysis of functionally graded sandwich plates", *Mech. Adv. Mater. Struct.*, **23**(4), 423-431. <https://doi.org/10.1080/15376494.2014.984088>.
- Cheraghbak, A., Dehkordi, M.B. and Golestanian, H. (2019), "Vibration analysis of sandwich beam with nanocomposite facesheets considering structural damping effects", *Steel Compos. Struct.*, **32**(6), 795-806. <https://doi.org/10.12989/scs.2019.32.6.795>.
- Ebrahimi, F. and Farazmandnia, N. (2018), "Vibration analysis of functionally graded carbon nanotube-reinforced composite sandwich beams in thermal environment", *Adv. Aircr. Spacecr. Sci.*, **5**(1), 107-128. <https://doi.org/10.12989/aas.2018.5.1.107>.
- Emdadi, M., Mohammadimehr, M. and Navi, B.R. (2019), "Free vibration of an annular sandwich plate with CNTRC facesheets and FG porous cores using Ritz method", *Adv. Nano Res.*, **7**(2), 109-123. <https://doi.org/10.12989/anr.2019.7.2.109>.
- Hadji, L. and Bernard, F. (2020), "Bending and free vibration analysis of functionally graded beams on elastic

- foundations with analytical validation”, *Adv. Mater. Res.*, **9**(1), 63-98.
<https://doi.org/10.12989/amr.2020.9.1.063>.
- Hadji, L. and Safa, A. (2020), “Bending analysis of softcore and hardcore functionally graded sandwich beams”, *Earthq. Struct.*, **18**(4), 481-492. <https://doi.org/10.12989/eas.2020.18.4.481>.
- Hadji, L., Atmane, H.A., Tounsi, A., Mechab, I. and Bedia, E.A. (2011), “Free vibration of functionally graded sandwich plates using four-variable refined plate theory”, *Appl. Math. Mech.*, **32**(7), 925-942.
<https://doi.org/10.1007/s10483-011-1470-9>.
- Hadji, L., Zouatnia, N. and Kassoul, A. (2017), “Wave propagation in functionally graded beams using various higher-order shear deformation beams theories”, *Struct. Eng. Mech.*, **62**(2), 143-149.
<https://doi.org/10.12989/sem.2017.62.2.143>.
- Hadji, L., Ait Amar Meziane, M. and Safa, A. (2018), “A new quasi-3D higher shear deformation theory for vibration of functionally graded carbon nanotube-reinforced composite beams resting on elastic foundation”, *Struct. Eng. Mech.*, **66**(6), 771-781. <https://doi.org/10.12989/sem.2018.66.6.771>.
- Hedayati, H. and Aragh, B.S. (2012), “Influence of graded agglomerated CNTs on vibration of CNT-reinforced annular sectorial plates resting on Pasternak foundation”, *Appl. Math. Comput.*, **218**(17), 8715-8735. <https://doi.org/10.1016/j.amc.2012.01.080>.
- Keddouri, A., Hadji, L., and Tounsi, A. (2019), “Static analysis of functionally graded sandwich plates with porosities”, *Adv. Mater. Res.*, **8**(3), 155-177. <https://doi.org/10.12989/amr.2019.8.3.155>.
- Khalili, S.M.R. and Mohammadi, Y. (2012), “Free vibration analysis of sandwich plates with functionally graded face sheets and temperature-dependent material properties: A new approach”, *Eur. J. Mech. A Solids.*, **35**, 61-74. <https://doi.org/10.1016/j.euromechsol.2012.01.003>.
- Khalili, S.M.R., Davar, A. and Fard, K.M. (2012), “Free vibration analysis of homogeneous isotropic circular cylindrical shells based on a new three-dimensional refined higher-order theory”, *Int. J. Mech. Sci.*, **56**(1), 1-25. <https://doi.org/10.1016/j.ijmecsci.2011.11.002>.
- Khelifa, Z., Hadji, L., Hassaine Daouadji, T. and Bourada, M. (2018), “Buckling response with stretching effect of carbon nanotube-reinforced composite beams resting on elastic foundation”, *Struct. Eng. Mech.*, **67**(2), 125-130. <https://doi.org/10.12989/sem.2018.67.2.125>.
- Mahi, A. and Tounsi, A. (2015), “A new hyperbolic shear deformation theory for bending and free vibration analysis of isotropic, functionally graded, sandwich and laminated composite plates”, *Appl. Math. Model.*, **39**(9), 2489-2508. <https://doi.org/10.1016/j.apm.2014.10.045>.
- Mohammadi, M., Ghayour, M. and Farajpour, A. (2013), “Free transverse vibration analysis of circular and annular graphene sheets with various boundary conditions using the nonlocal continuum plate model”, *Compos. Part B Eng.*, **45**(1), 32-42. <https://doi.org/10.1016/j.compositesb.2012.09.011>.
- Murmu, T., McCarthy, M.A. and Adhikari, S. (2013), “In-plane magnetic field affected transverse vibration of embedded single layer graphene sheets using equivalent nonlocal elasticity approach”, *Compos. Struct.*, **96**, 57-63. <https://doi.org/10.1016/j.compstruct.2012.09.005>.
- Natarajan, S., Haboussi, M. and Manickam, G. (2014), “Application of higher-order structural theory to bending and free vibration analysis of sandwich plates with CNT reinforced composite facesheets”, *Compos. Struct.*, **113**, 197-207. <https://doi.org/10.1016/j.compstruct.2014.03.007>.
- Pourmoayed, A.R., Malekzadeh Fard, K. and Shahravi, M. (2017), “Vibration analysis of a cylindrical sandwich panel with flexible core using an improved higher-order theory”, *Latin Am. J. Solids Struct.*, **14**(4), 714-742. <https://doi.org/10.1590/1679-78253410>.
- Qatu M.S. (2004), *Vibration of Laminated Shells and Plates*, Elsevier Academic Press, Amsterdam, Netherlands.
- Reddy, J.N. (2003), *Mechanics of Laminated Composite Plates and Shells: Theory and Analysis*, CRC press, Florida, USA.
- Safa, A., Hadji, L., Bourada, M. and Zouatnia, N. (2019), “Thermal vibration analysis of FGM beams using an efficient shear deformation beam theory”, *Earthq. Struct.*, **17**(3), 329-336.
<https://doi.org/10.12989/eas.2019.17.3.329>.
- Shen, H.S. (2009), “Nonlinear bending of functionally graded carbon nanotube-reinforced composite plates in thermal environments”, *Compos. Struct.*, **91**(1), 9-19. <https://doi.org/10.1016/j.compstruct.2009.04.026>.

- Wang, Z.X. and Shen, H.S. (2012), "Nonlinear vibration and bending of sandwich plates with nanotube-reinforced composite fnonlinear", *Compos. Part B Eng.*, **43**(2), 411-421.
<https://doi.org/10.1016/j.compositesb.2011.04.040>.
- Zine, A., Tounsi, A., Draiche, K., Sekkal, M. and Mahmoud, S.R. (2018), "A novel higher-order shear deformation theory for bending and free vibration analysis of isotropic and multilayered plates and shells", *Steel Compos. Struct.*, **26**(2), 125-137. <https://doi.org/10.12989/scs.2018.26.2.125>.
- Zouatnia, N. and Hadji, L. (2019), "Static and free vibration behavior of functionally graded sandwich plates using a simple higher order shear deformation theory", *Adv. Mater. Res.*, **8**(4), 313-335.
<https://doi.org/10.12989/amr.2019.8.4.313>.
- Zouatnia, N., Hadji, L. and Kassoul, A., (2017), "An analytical solution for bending and vibration responses of functionally graded beams with porosities", *Wind Struct.*, **25**(4), 329-342.
<https://doi.org/10.12989/was.2017.25.4.329>.

CC

Appendix A

$$\begin{aligned}
 N_x^p &= A_{11}^p \frac{\partial u_{0p}}{\partial x} + B_{11}^p \frac{\partial u_{1p}}{\partial x} + C_{11}^p \frac{\partial u_{2p}}{\partial x} + D_{11}^p \frac{\partial u_{3p}}{\partial x} + A_{12}^p \frac{\partial v_{0p}}{\partial y} + B_{12}^p \frac{\partial v_{1p}}{\partial y} + C_{12}^p \frac{\partial v_{2p}}{\partial y} + \\
 &D_{12}^p \frac{\partial v_{3p}}{\partial y} + A_{13}^p w_1 + 2B_{13}^p w_2 + A_{16}^p \left(\frac{\partial u_{0p}}{\partial y} + \frac{\partial v_{0p}}{\partial x} \right) + B_{16}^p \left(\frac{\partial u_{1p}}{\partial y} + \frac{\partial v_{1p}}{\partial x} \right) + C_{16}^p \times \\
 &\left(\frac{\partial u_{2p}}{\partial y} + \frac{\partial v_{2p}}{\partial x} \right) + D_{16}^p \left(\frac{\partial u_{3p}}{\partial y} + \frac{\partial v_{3p}}{\partial x} \right) + Z_{31}^p \phi^p(x, y, t) \\
 N_{xy}^p &= A_{66}^p \left(\frac{\partial u_{0p}}{\partial y} + \frac{\partial v_{0p}}{\partial x} \right) + B_{66}^p \left(\frac{\partial u_{1p}}{\partial y} + \frac{\partial v_{1p}}{\partial x} \right) + C_{66}^p \left(\frac{\partial u_{2p}}{\partial y} + \frac{\partial v_{2p}}{\partial x} \right) + D_{66}^p \left(\frac{\partial u_{3p}}{\partial y} + \frac{\partial v_{3p}}{\partial x} \right) \\
 M_y^p &= B_{12}^p \frac{\partial u_{0p}}{\partial x} + C_{12}^p \frac{\partial u_{1p}}{\partial x} + D_{12}^p \frac{\partial u_{2p}}{\partial x} + E_{12}^p \frac{\partial u_{3p}}{\partial x} + B_{22}^p \frac{\partial v_{0p}}{\partial y} + C_{22}^p \frac{\partial v_{1p}}{\partial y} + D_{22}^p \frac{\partial v_{2p}}{\partial y} + \\
 &E_{22}^p \frac{\partial v_{3p}}{\partial y} + B_{23}^p w_1 + 2C_{23}^p w_2 + B_{26}^p \left(\frac{\partial u_{0p}}{\partial y} + \frac{\partial v_{0p}}{\partial x} \right) + C_{26}^p \left(\frac{\partial u_{1p}}{\partial y} + \frac{\partial v_{1p}}{\partial x} \right) + D_{26}^p \\
 &\left(\frac{\partial u_{2p}}{\partial y} + \frac{\partial v_{2p}}{\partial x} \right) + E_{26}^p \left(\frac{\partial u_{3p}}{\partial y} + \frac{\partial v_{3p}}{\partial x} \right) + Z_{32}^p \phi^p(x, y, t) \\
 P_{xy}^p &= C_{66}^p \left(\frac{\partial u_{0p}}{\partial y} + \frac{\partial v_{0p}}{\partial x} \right) + D_{66}^p \left(\frac{\partial u_{1p}}{\partial y} + \frac{\partial v_{1p}}{\partial x} \right) + E_{66}^p \left(\frac{\partial u_{2p}}{\partial y} + \frac{\partial v_{2p}}{\partial x} \right) + F_{66}^p \left(\frac{\partial u_{3p}}{\partial y} + \frac{\partial v_{3p}}{\partial x} \right) \\
 R_{xy}^p &= D_{66}^p \left(\frac{\partial u_{0p}}{\partial y} + \frac{\partial v_{0p}}{\partial x} \right) + E_{66}^p \left(\frac{\partial u_{1p}}{\partial y} + \frac{\partial v_{1p}}{\partial x} \right) + F_{66}^p \left(\frac{\partial u_{2p}}{\partial y} + \frac{\partial v_{2p}}{\partial x} \right) + G_{66}^p \left(\frac{\partial u_{3p}}{\partial y} + \frac{\partial v_{3p}}{\partial x} \right) \\
 &p = t, c, b
 \end{aligned} \tag{A1}$$

Appendix B

$$\delta \lambda_1 u_{0t} + \frac{h_t}{2} u_{1t} + \left(\frac{h_t}{2} \right)^2 u_{2t} + \left(\frac{h_t}{2} \right)^3 u_{3t} - u_{0c} + \frac{h_c}{2} u_{1c} - \left(\frac{h_c}{2} \right)^2 u_{2c} + \left(\frac{h_c}{2} \right)^3 u_{3c} = 0 \tag{B1}$$

$$\begin{aligned}
& \delta\lambda_5 w_{0t} + \frac{h_t}{2} w_{1t} + \left(\frac{h_t}{2}\right)^2 w_{2t} - w_{0c} + \frac{h_c}{2} w_{1c} - \left(\frac{h_c}{2}\right)^2 w_{2c} = 0 \\
& \delta\lambda_{10} \frac{\partial w_{0b}}{\partial x} + (h_b/2) \frac{\partial w_{1b}}{\partial x} + (h_b/2)^2 \frac{\partial w_{2b}}{\partial x} + u_{1b} + h_b u_{2b} + 3(h_b/2)^2 u_{3b} = 0 \\
& \delta\lambda_{16} Q_{55}^b \left(\frac{\partial w_{0b}}{\partial x} + \left(-\frac{h_b}{2}\right) \frac{\partial w_{1b}}{\partial x} + \left(\frac{h_b}{2}\right)^2 \frac{\partial w_{2b}}{\partial x} + u_{1b} - h_b u_{2b} + 3\left(\frac{h_b}{2}\right)^2 u_{3b} \right) - G_{xz}^c \\
& \left(\frac{\partial w_{0c}}{\partial x} + (h_c/2) \frac{\partial w_{1c}}{\partial x} + (h_c/2)^2 \frac{\partial w_{2c}}{\partial x} + u_{1c} + h_c u_{2c} + 3(h_c/2)^2 u_{3c} \right) = 0
\end{aligned}$$

Appendix C

$$\begin{aligned}
\lambda_1(x, y, t) &= \sum_{m=1}^{\infty} \sum_{n=1}^{\infty} \lambda_1^{mn} e^{i\omega t} \sin(n\pi y/b) \cos(m\pi x/a) \\
\lambda_3(x, y, t) &= \sum_{m=1}^{\infty} \sum_{n=1}^{\infty} \lambda_3^{mn} e^{i\omega t} \cos(n\pi y/b) \sin(m\pi x/a) \\
\lambda_8(x, y, t) &= \sum_{m=1}^{\infty} \sum_{n=1}^{\infty} \lambda_8^{mn} e^{i\omega t} \sin(n\pi y/b) \cos(m\pi x/a) \\
\lambda_{11}(x, y, t) &= \sum_{m=1}^{\infty} \sum_{n=1}^{\infty} \lambda_{11}^{mn} e^{i\omega t} \sin(n\pi y/b) \sin(m\pi x/a) \\
\lambda_{15}(x, y, t) &= \sum_{m=1}^{\infty} \sum_{n=1}^{\infty} \lambda_{15}^{mn} e^{i\omega t} \cos(n\pi y/b) \sin(m\pi x/a) \\
\lambda_{16}(x, y, t) &= \sum_{m=1}^{\infty} \sum_{n=1}^{\infty} \lambda_{16}^{mn} e^{i\omega t} \sin(n\pi y/b) \cos(m\pi x/a)
\end{aligned} \tag{C1}$$